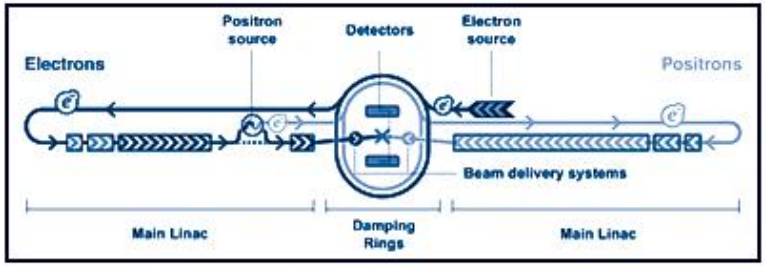

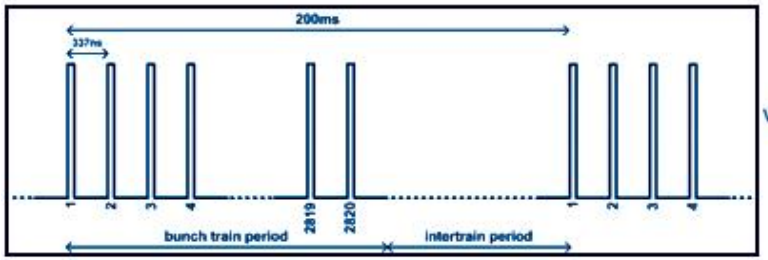

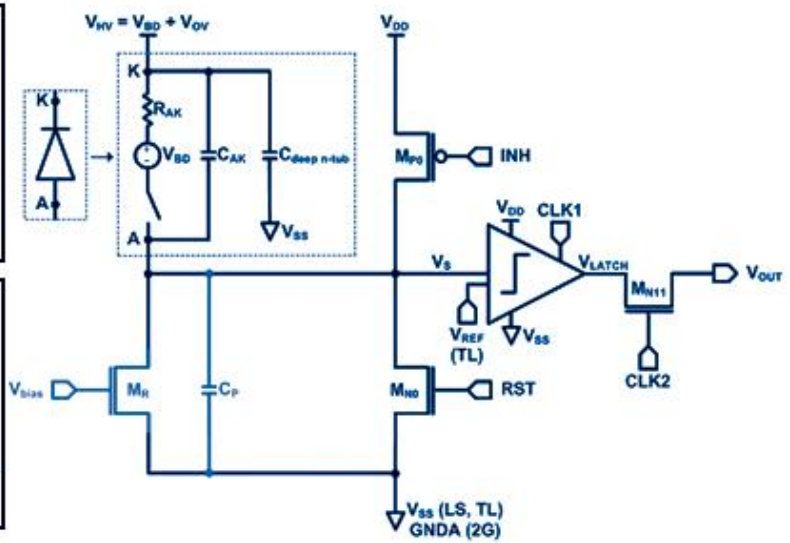

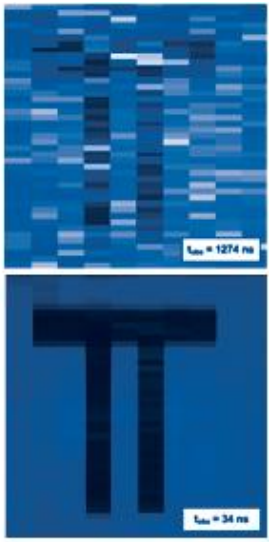

SPADs FOR VERTEX TRACKER DETECTORS IN FUTURE COLLIDERS

Angel Diéguez.
Department of Electronics, University of Barcelona

Thanks to the Spanish FPA program for financing of projects FPA2008-05979 and FPA2010-21549 and the CEE for the Advanced European Infrastructures for Detectors at Accelerators FP7 contract.

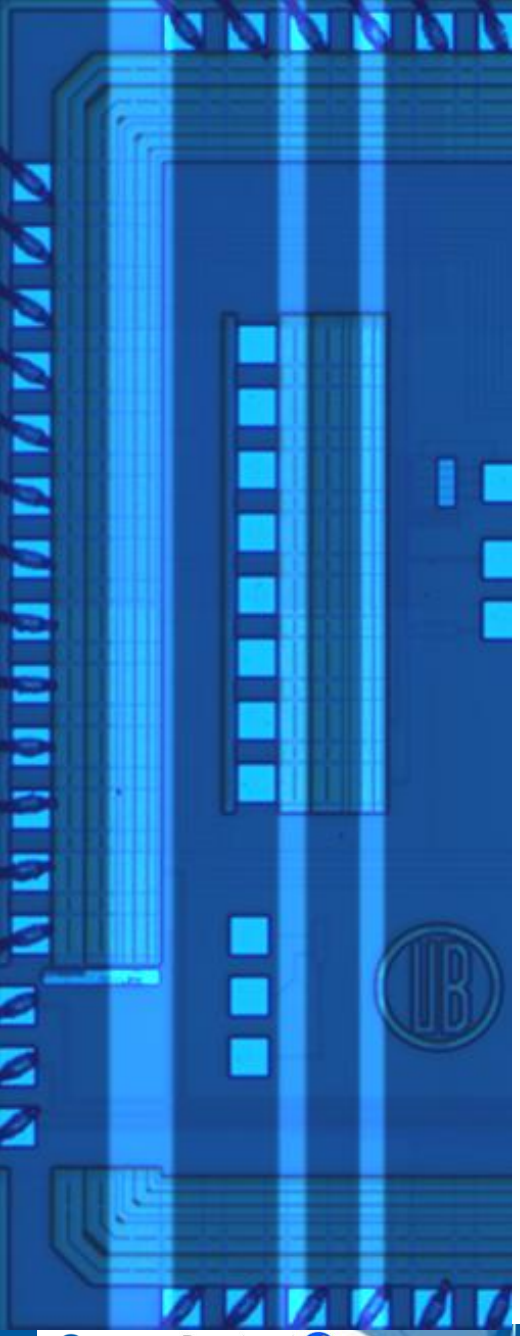

OUTLINE

INTRODUCTION

SPAD DEVICE
Operation
Realization

SPADs FOR TRACKERs

CONCLUSIONS

INTRODUCTION

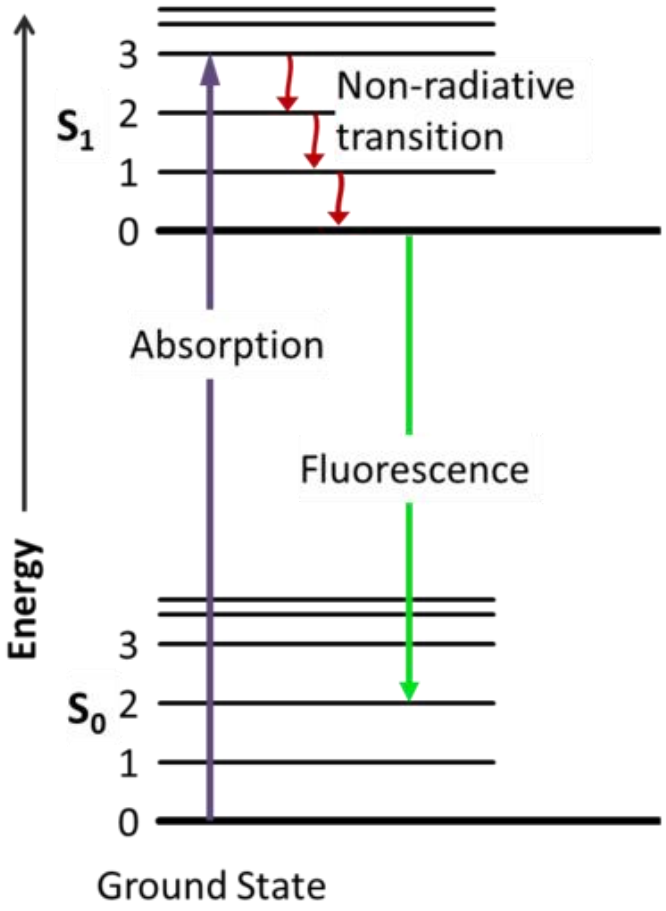

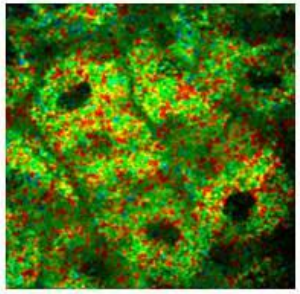

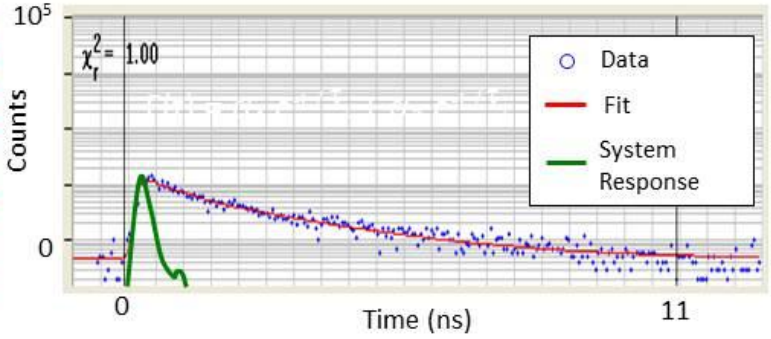

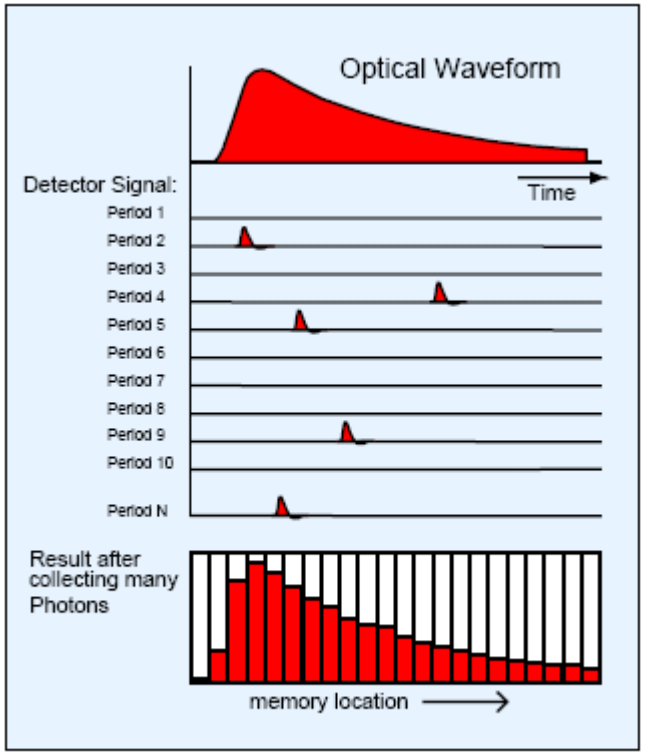

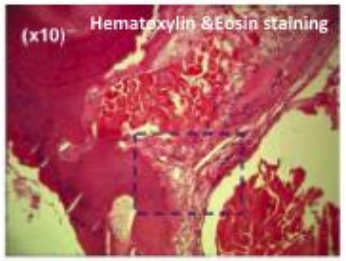

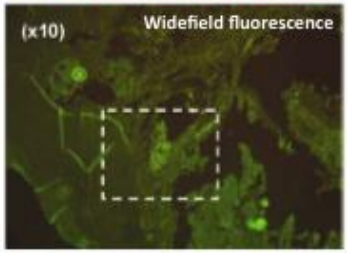

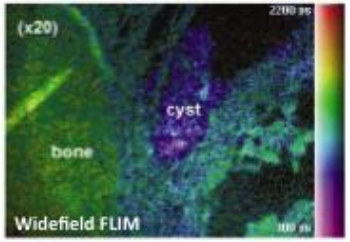

Time-correlated single photon counting

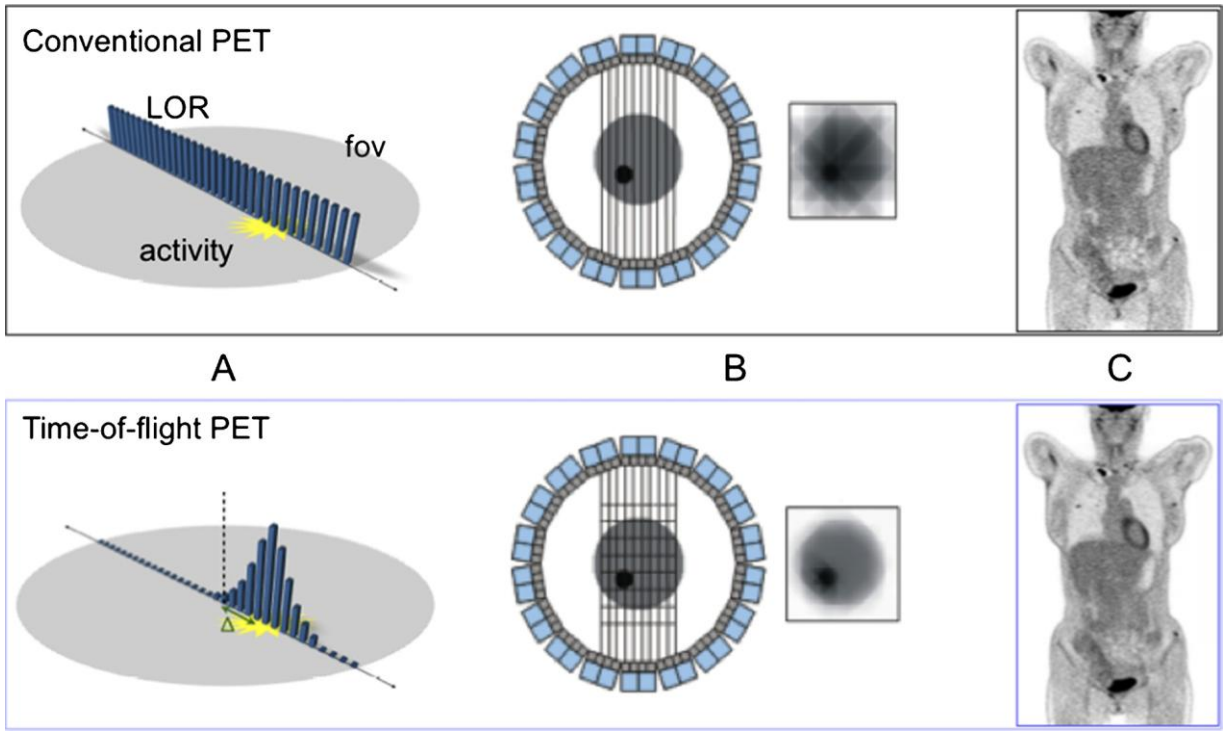

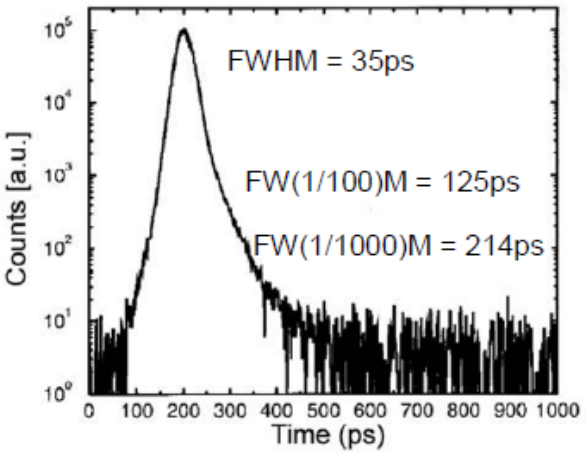

A.Spinelli, M.Ghioni, S.Covaand L.M.Davis, IEEE J.Quantum Electron. QE-34, 817 (1998)

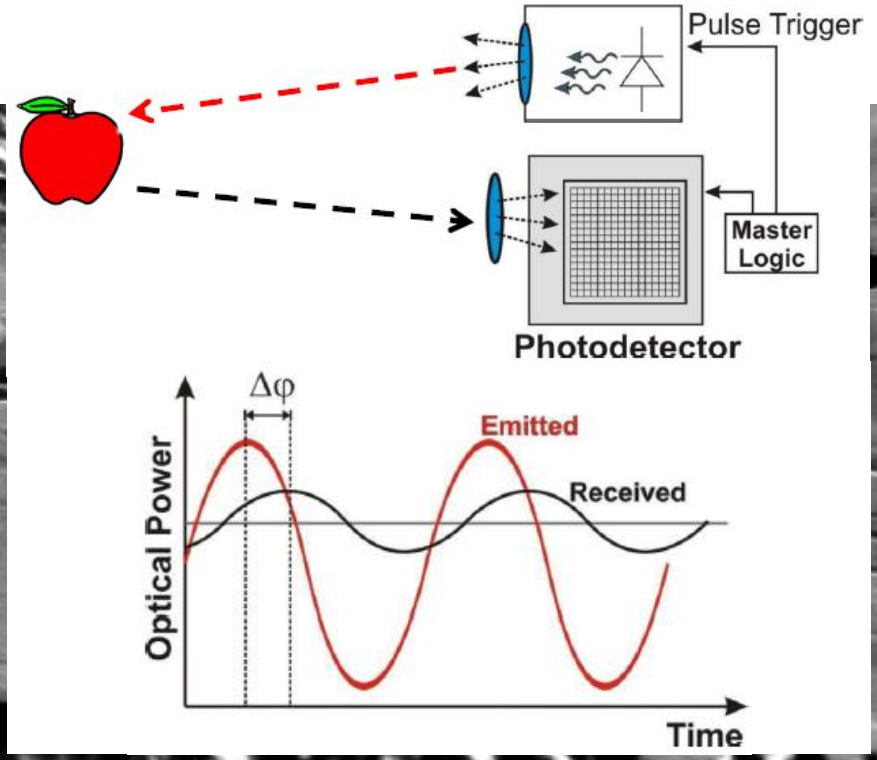
Pulse Trigger
Master Logic
Photodetector
Δφ
Emitted
Received
Optical Power
Time

Tracking: Reconstructing charged particles trajectory taking several position measurements (sometimes also time) as particle passes through the detector.

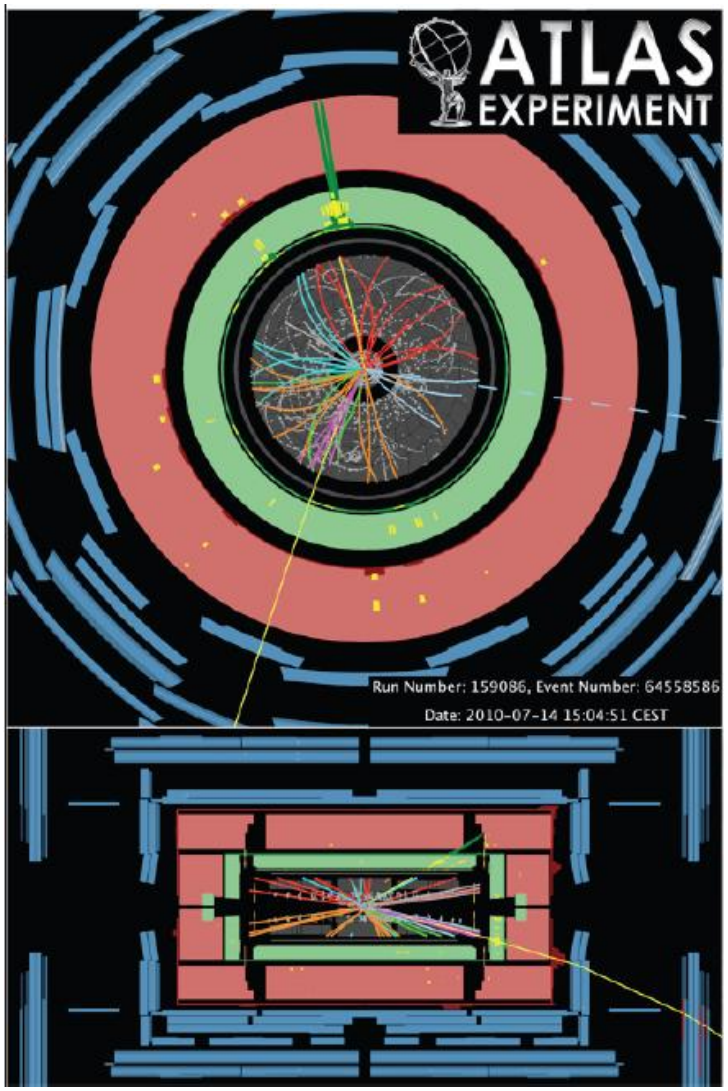

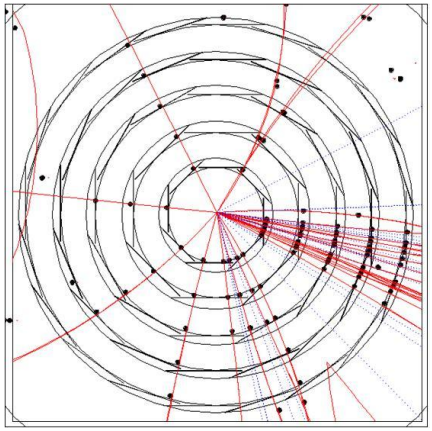

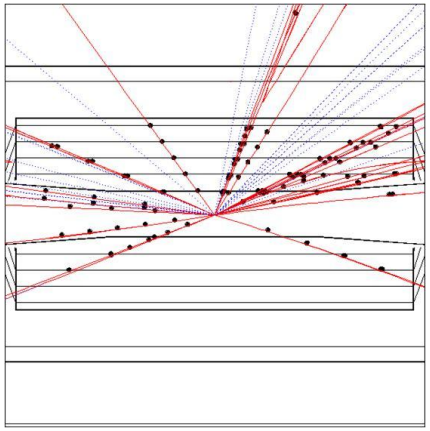

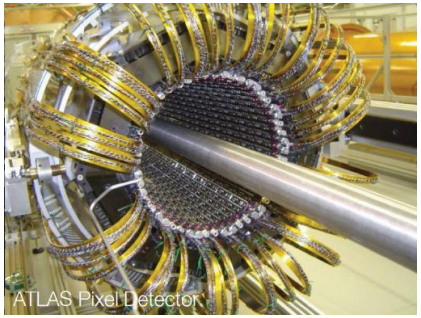

Why Avalanche Photodiodes (geiger) for tracking?

For measuring particle hit is not necessary a signal proportional to the charge (APD-lineal, SiPM). Usually time measurement is not needed (APD with TDC).

- Performance:
  - Very high gain in the sensor (Single-photon sensitivity for light)
  - Fast response (fits in single BX for some future colliders)

- Implementation:
  - Intrinsically digital sensor: simple readout
  - Possible in CMOS technology: simple design, detection in ~1-2μm (thinning)

Questions to answer:
SPADs detect all particles? (sensitivity)
Noise? (design, technology)
Can cover >90% detection area? (fill factor, design)
…

SPAD DEVICE

Introduction to avalanche photodiode concept

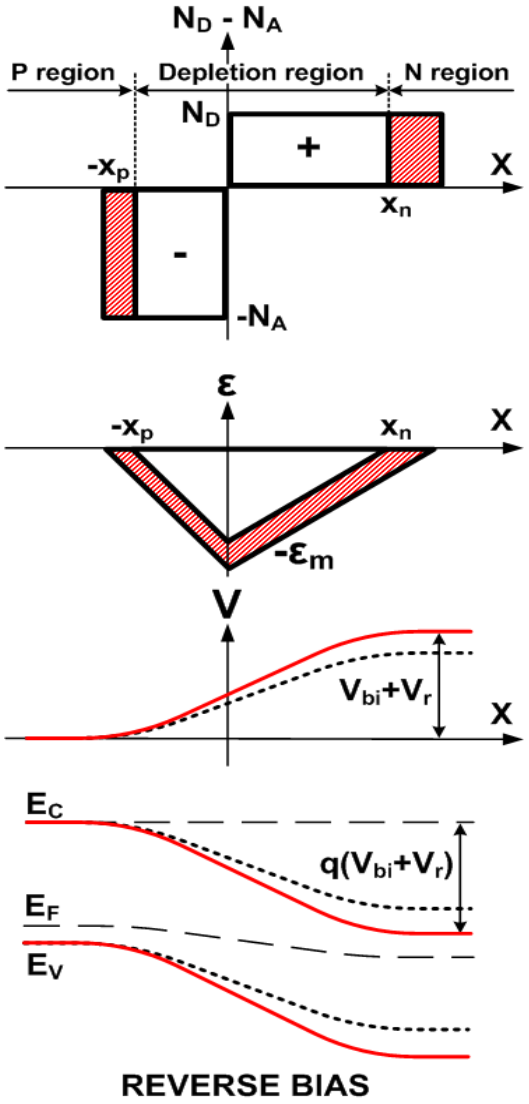

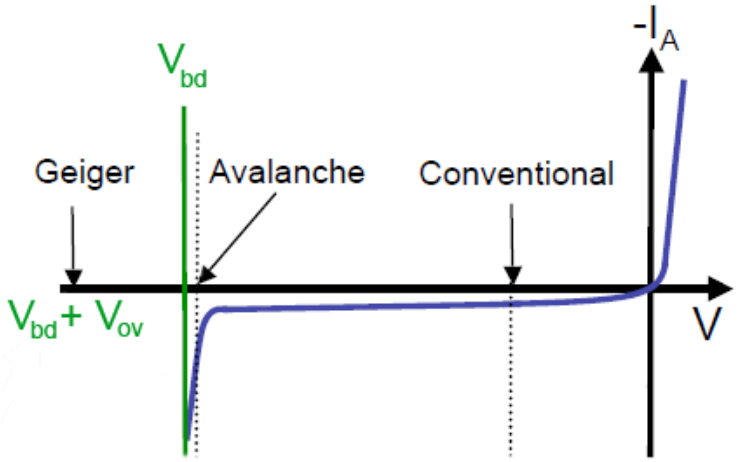

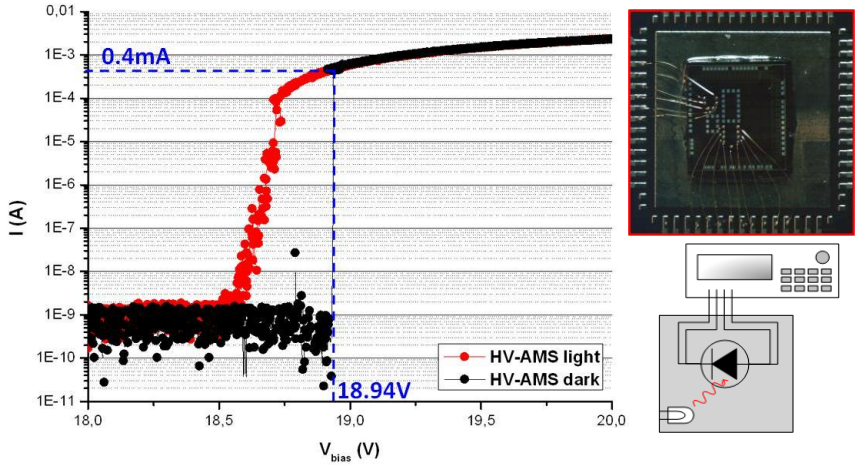

A. Arbat, PhD, Towards a forward tracker detector based on Geiger mode avalanche photodiodes for future linear colliders, 2010.

Introduction to avalanche photodiode concept

Avalanche generation:

- Geiger mode: High E
  - Electrons and holes
  - Self sustained

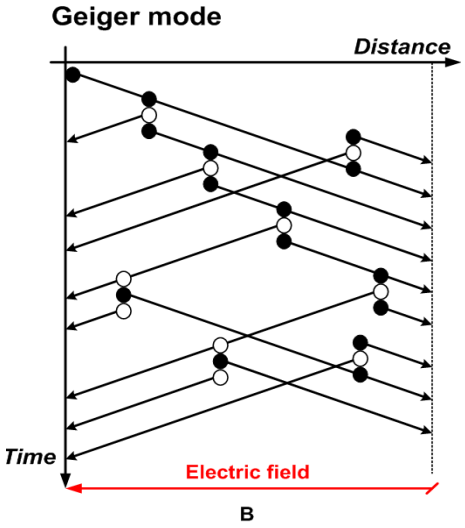

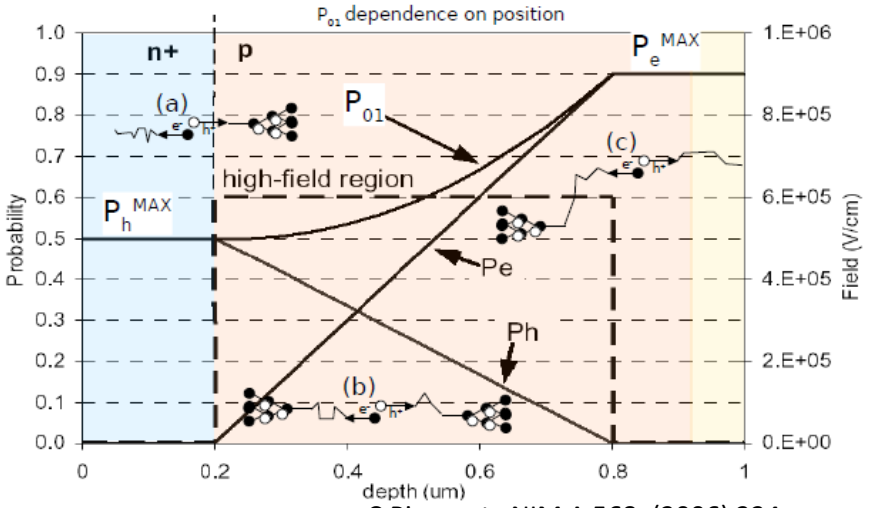

C.Piemonte NIM A 568, (2006) 224

e-h pair generation due to:

- External interaction:
  - Photon absoption.

  PDE = QE * P_{01} * ε
  - Minimum Ionizing Particle
- Noise:
  - Dark counts: Thermal release of charge, tunnel effect
  - Afterpulses
  - Cross-talk

• in dedicated technology 0.1~1Hz/µm²
• in CMOS SPADs 1~10Hz/µm²

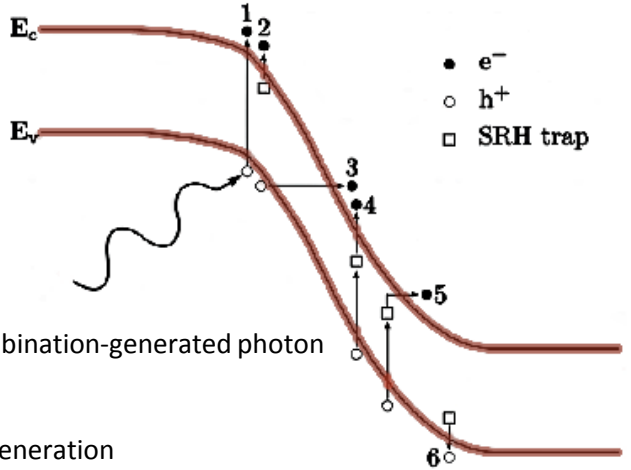

1) cross-talk from a recombination-generated photon
2) Electron afterpulsing
3) Band to band tunneling
4) Trap-assisted thermal generation
5) Trap-assisted tunneling
6) Hole afterpulsing

Fishburn, PhD 2012.

Implementation of avalanche photodiodes

Haitz's planar diode (early 60's)

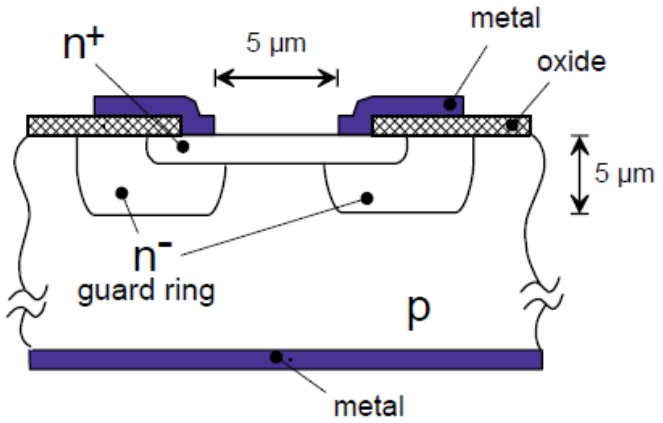

R.Haitz, J.Appl.Phys. 35, 1370 (1964), J.Appl.Phys. 36, 3123 (1965)

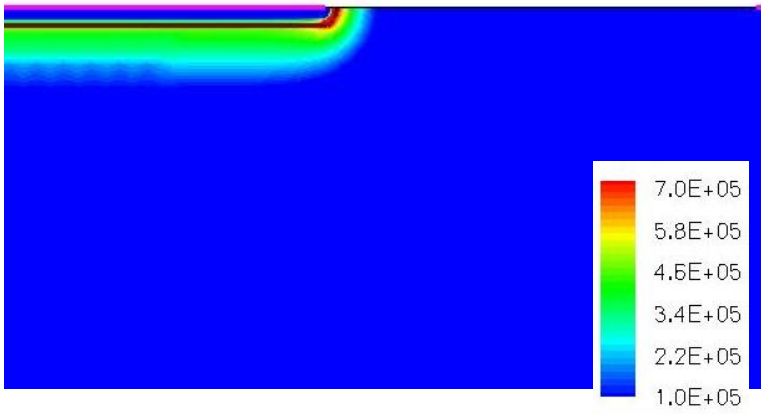

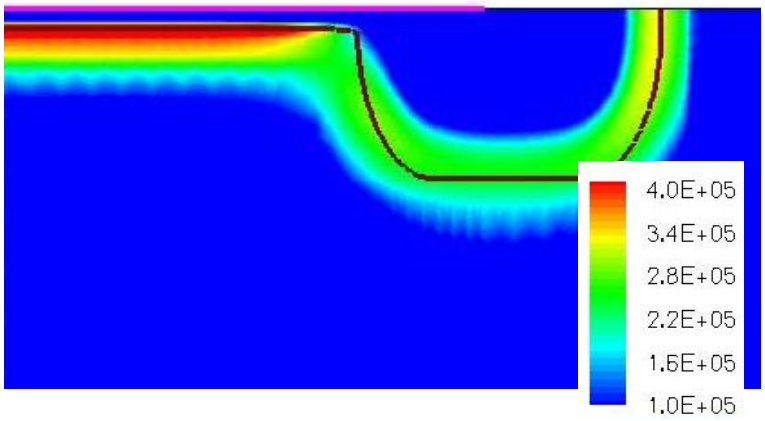

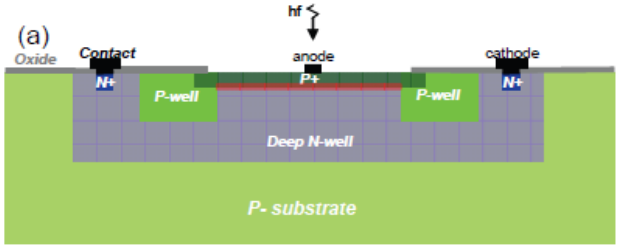

Goetzberger, 1963; Cova,1981; Kindt, 1994; custom
Rochas, 2002, CMOS 0.8; Niclass, 2007, CMOS 0.13;
Arbat, 2008, CMOS 0.35, Vilella 2009, CMOS 0.35

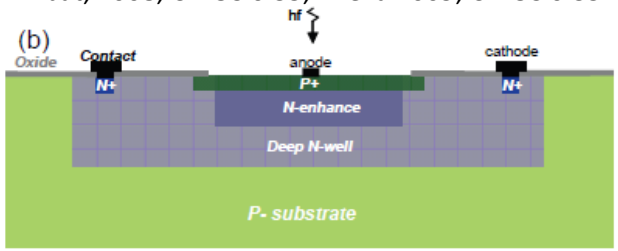

Petrillo, 1984; Ghioni, 1988, Lacaita, 1989, custom
Pancheri, 2007 CMOS 0.7

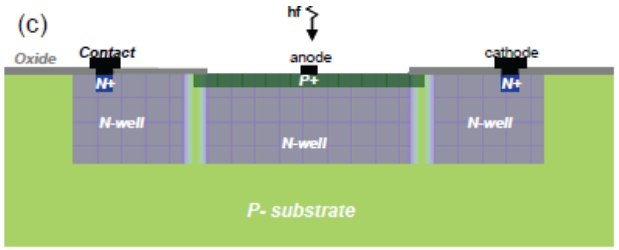

Pauchard, 2000; custom
Rochas, 2001, CMOS 0.8

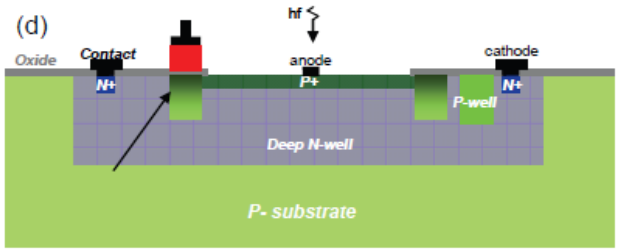

Rochas, 2003, CMOS 0.8; Xiao, 2007, CMOS 0.35

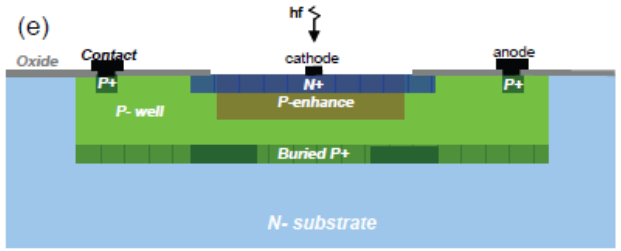

Cova, 1981; Ghioni, 1988, Lacaita, 1989; custom

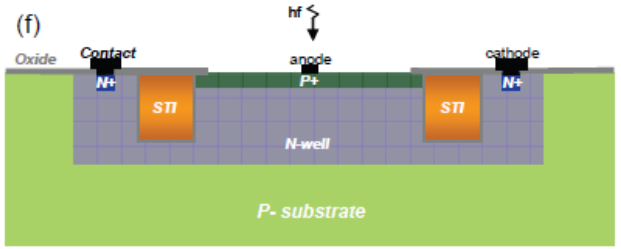

Finkelstein , 2006,CMOS 0.18; Hsu, 2009, CMOS 0.18;
Niclass, 2007, CMOS 0.13; Gersback, 2008, CMOS 0.13,
Arbat, 2008, CMOS 0.13

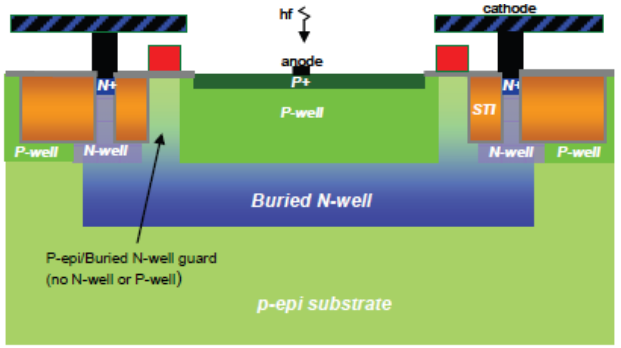

Richardson, 2009, CMOS 0.13, Webster, 2012, CMOS 0.09

G.F.Dalla Betta, “Avalanches in Photodiodes” Ed., InTech Pub. (2011)

Implementation of avalanche photodiodes

Reference	J. Richardson 2009	M. Gersbach 2009	C. Niclass 2007
Active area	50.3 mm^2	58 mm^2	53 mm^2
Type	p^+/p-well/buried n-well	p^+/n-well	p^+/n-well
Guard ring	buried n-well with poly gate	STI with p-type passivation	p-well/STI with poly gate
V_{BD}	14.3V	9.4V	9.7V
DCR	40Hz@V_{ex}=1V	670kHz@V_{ex}=2V	100kHz@V_{ex}=1.7V
PDE	28%@ 500nm	30%@480nm	34%@450nm
Jitter	184ps FWHM	125ps FWHM	144 ps FWHM
Afterpulsing	0.02%@T_D=100ns	<1%@T_D=180ns	n.a.

D. Stoppa – New Challenges for CMOS Imagers – Delft December 1st 2010

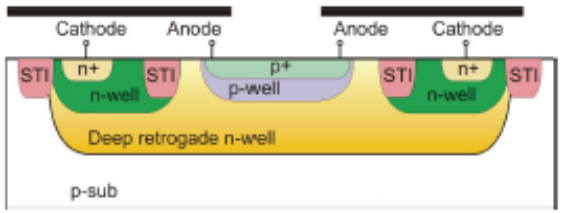

Richardson'09

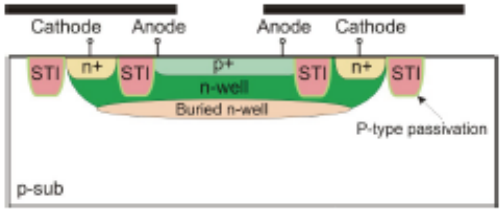

Gersbach'09

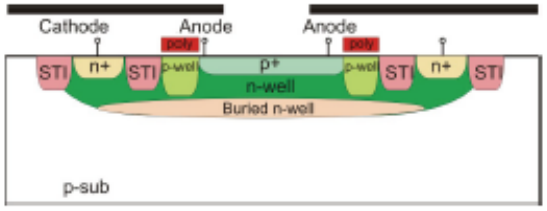

Niclass'07

(1) Niclass et al., IEEE J. Quantum Electronics 13(4), 2007.
(2) Gersbach et al., Solid-State Electronics 53(7), 2009
(3) Richardson et al., Int. Image Sensor Workshop, 2009

Implementation of avalanche photodiodes

Custom

Excellent PDE and timing properties

Low DCR and afterpulsing

Bigger pixels possible

Not suitable in arrays

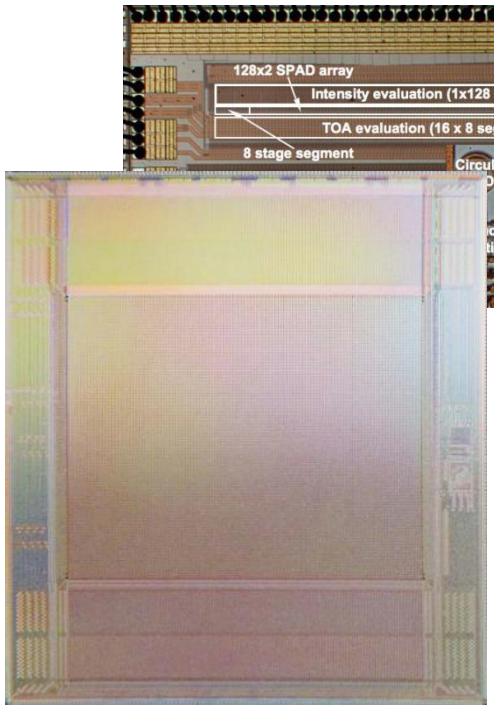

Charbon, group

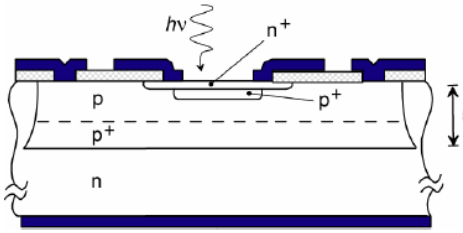

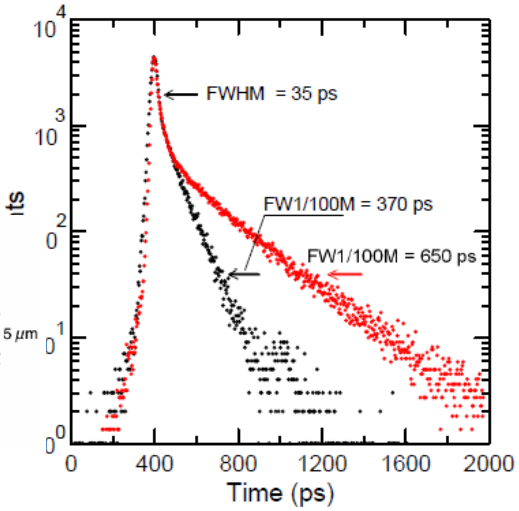

G. Ripamontiand S. Cova, Solid State Electron. 28, 925 (1985)
M.Ghioni, S.Cova, A.Lacaita, G.Ripamonti, Electron. Lett. 24, 1476 (1988)
A.Lacaita, M.Ghioni, S.Cova, Electron.Lett. 25, 841 (1989)

CMOS

Possible complex arrays of smart pixels. In-pixel electronics.

Shallow implants, high doping

- acceptable PDE
- moderate DCR, high with STI

Very good timing resolution (long diffusion tails)

Smaller sizes demonstrated

Better tunning, DCR with flash extension in HV processes (deep well)

APD operation, quenching and recharge circuits

Passive quenching and recharge

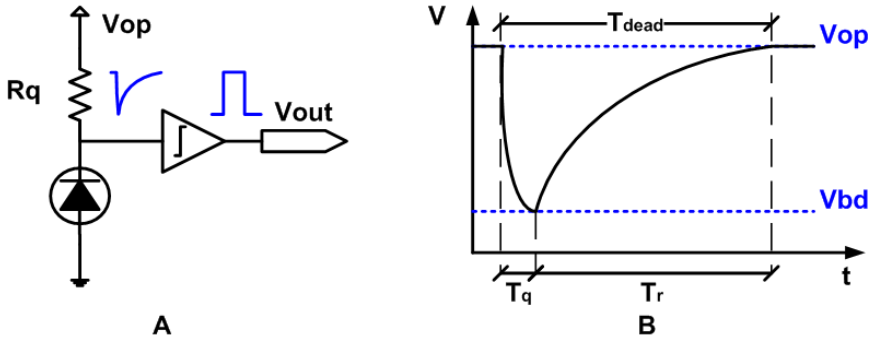

Active quenching and passive recharge

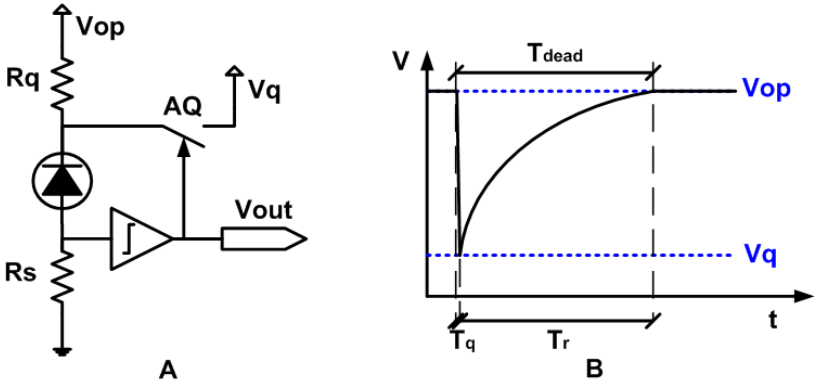

Passive quenching and active recharge

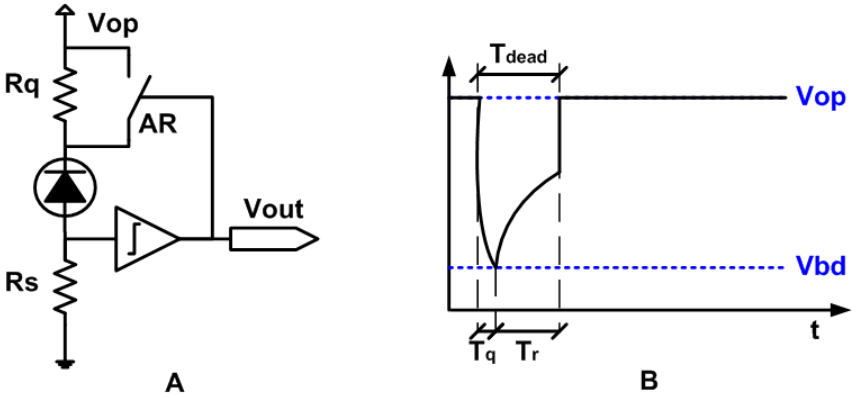

Active quenching and recharge

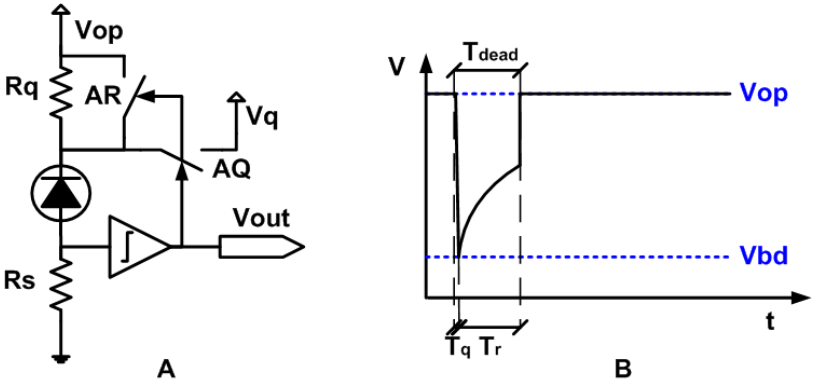

P. Antognetti et al. 1975 “A study of the operation and performances of an avalanche diode as a single photon detector”

S. Cova et al. 1981 “Towards picosecond resolution with single-photon avalanche diodes”

S. Cova et al. 1996 “Avalanche photodiodes and quenching circuits for single-photon detection”

APD operation, free running and gated mode

Free running:

The APD is always in operation condition

Gated mode:

The APD is in observation for short periods of time:

- applications where the signal time arrival can be known in advance
- the SPAD is kept active only for short periods that can be synchronized with the expected signal
- reduces the dark count
- improves the detection efficiency
- avoids afterpulsing

Two possible circuits:

A) dc coupling

B) ac coupling

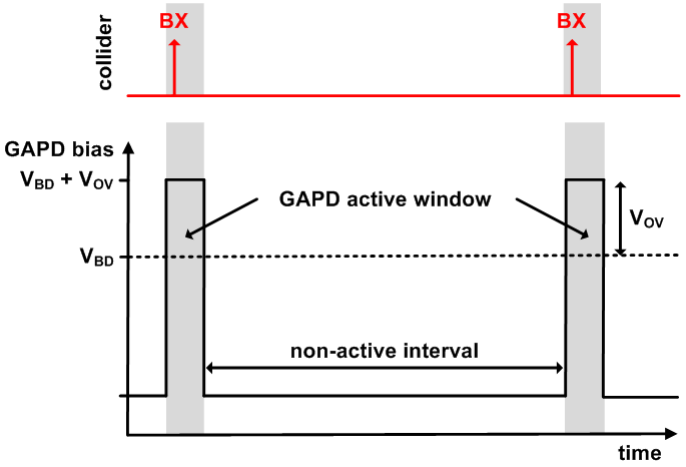

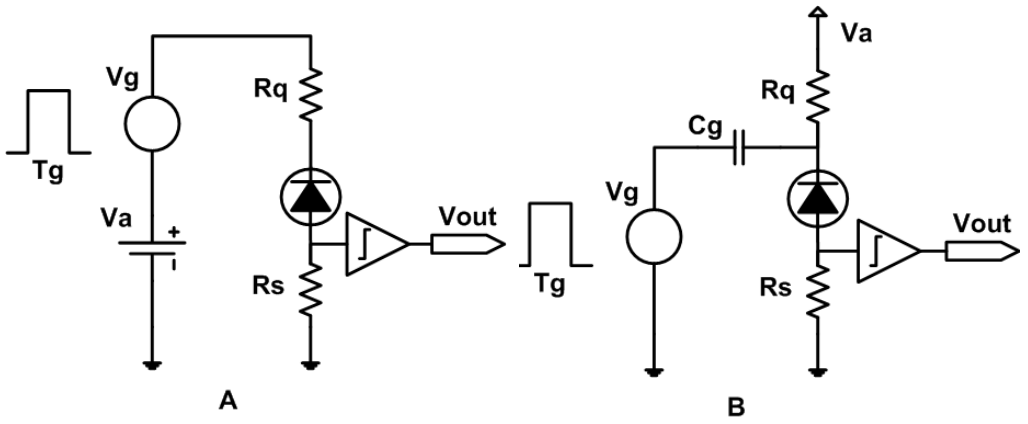

S. Cova et al. 1996 "Avalanche photodiodes and quenching circuits for single-photon detection"

Random access, full camera readout

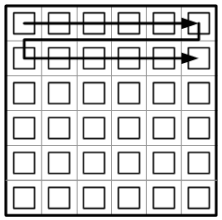

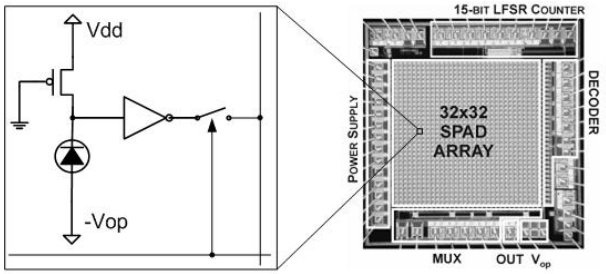

C. Niclass et al. 2005 "A single photon detector array with 64x64 resolution and millimetric depth accuracy for 3D imaging", *2005: Ø 7μm Pitch 58μm → 32 x 32; 0.8μm*

Event driven readout, few pixels read

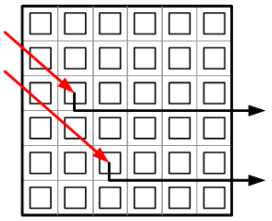

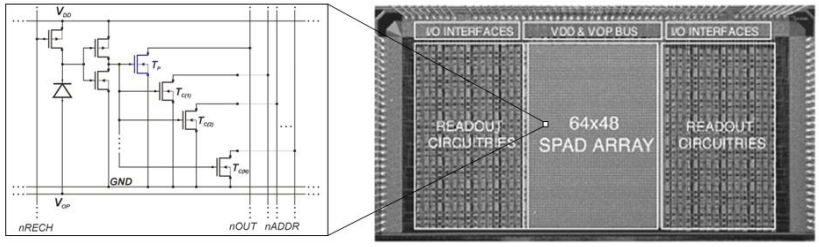

C. Niclass et al. 2007 "A CMOS 64x48 single photon avalanche diode array with event-driven readout", 2006: Ø 7μm Pitch 45μm→ 64 x 48; 0.8μm

Parallel readout, full camera readout

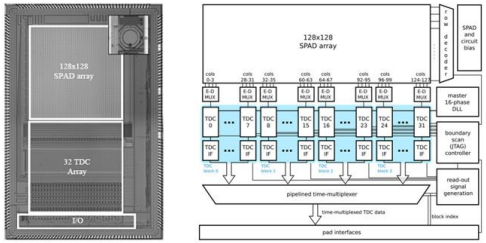

C. Niclass et al. 2008 "A 128x128 single-photon imager with on-chip column-level 10b time-to-digital converter array capable of 97ps resolution", 2008: Pitch 25μm → 128 x 128; 0.35 μm

In-pixel storing, full camera readout

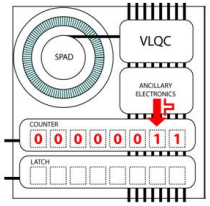

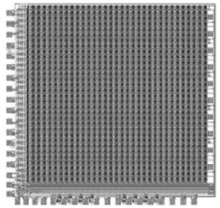

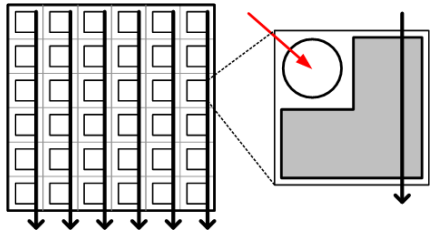

F. Guerrieri et al. 2008 "Fast single-photon imager acquires 1024 pixels at 100 kframe/s", 2008: Φ 20μm Pitch 100μm → 32 x 32; 0.35 μm

Pipelined readout

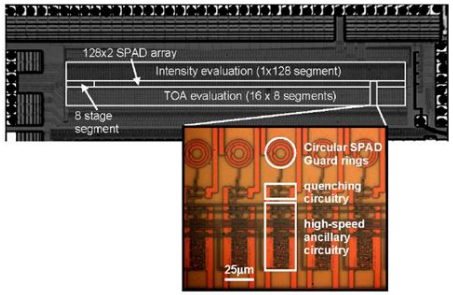

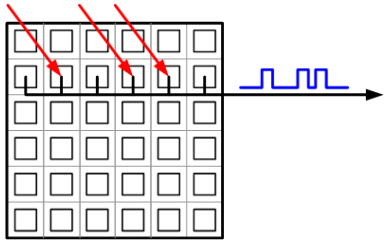

M. Sergio et al. 2007 "A 128x2 CMOS single photon streak camera with timing-preserving latchless pipeline readout", 2007: Pitch 25μm x 110μm→ 128 x 2; 0.35μm

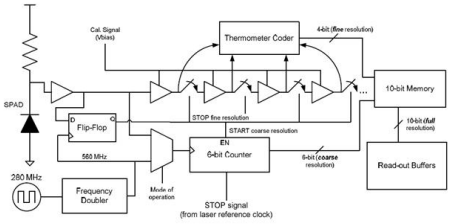

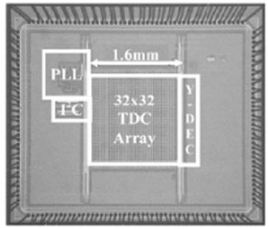

M. Gersbach et al. 2009 "A parallel 32x32 time-to-digital converter array fabricated in a 130nm imaging CMOS technology", 2009: Pitch 50x50μm² → 32 x 32; 0.13 μm

SPADs FOR TRACKERs

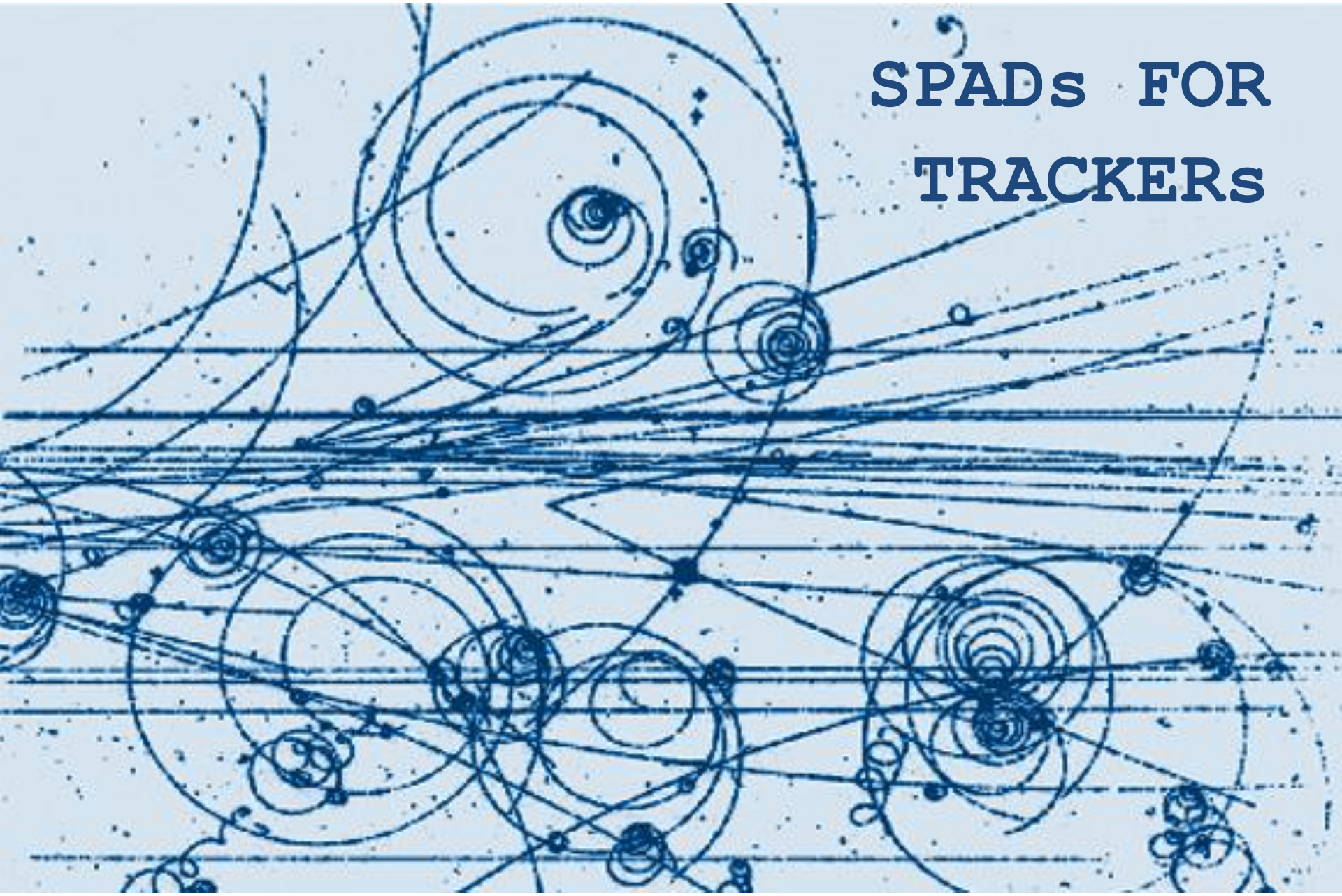

Beam structure, two examples ILC and CLIC

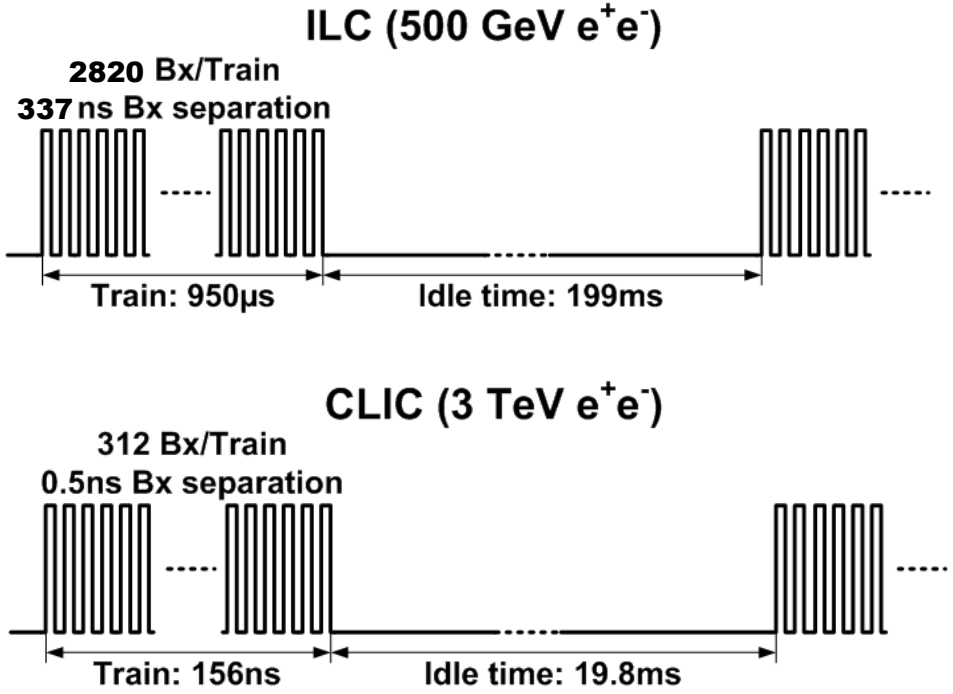

Detector requirements, FTD ILC

- Very low mass: 0.1% X_0 per layer (equivalent of 100 μm of Si)
- High resolution: impact parameter resolution of ~ 5 μm (pixel size ~ 20 μm)
- Good and robust pattern recognition, integrated design, bunch crossing time stamp
- Modest radiation tolerance for ILC applications <100kRad/year
- ILC, Innermost vertex layer has ~ 0.06 hits/mm^2/BX, FTD D4 background ~ $2\cdot10^{-4}$ hits/mm^2/BX
  ~ $6\cdot10^{-8}$ hits/um^2/BX, ~ $2\cdot10^{-10}$ hits/um^2/BX

SPADs for trackers, 10x43 GAPD array oriented to ILC

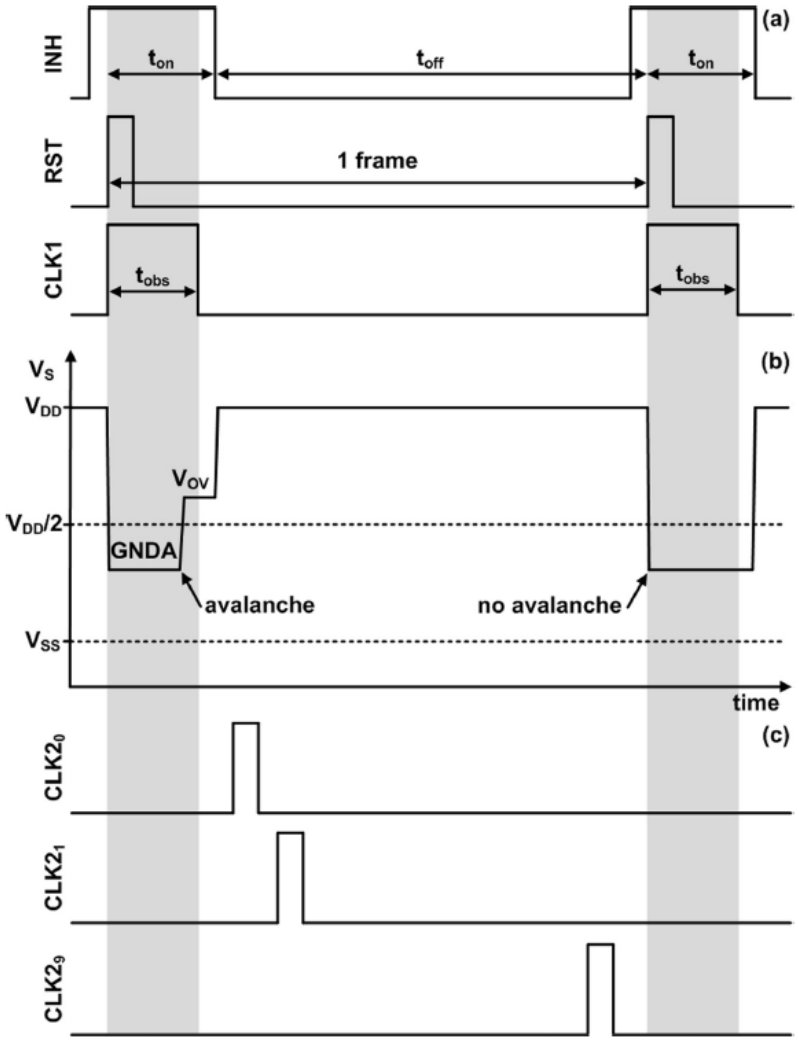

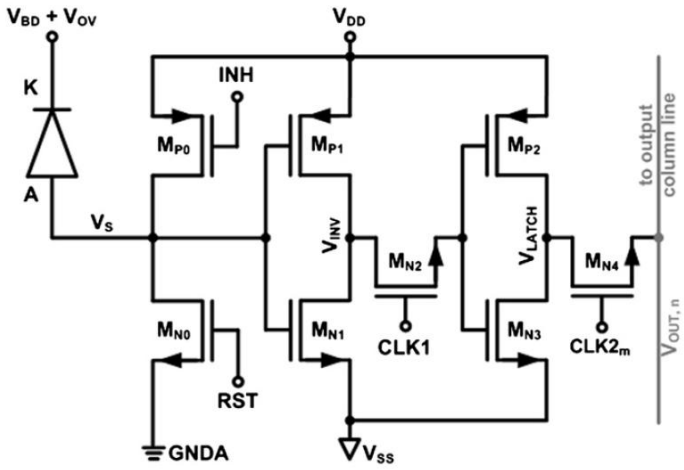

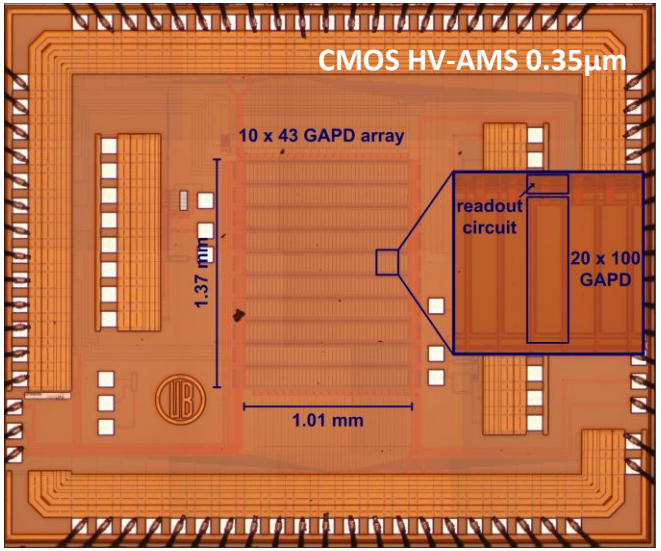

E. Vilella et al., A gated single-photon avalanche diode array fabricated in a conventional CMOS process for triggered systems, Sensors & Actuators A 186, 2012

E. Vilella et al., A low-noise time-gated single-photon detector in a HV-CMOS technology for triggered imaging , Sensors &Actuators A 201, 2013.

High energy particle detection (1)

- **Series of beam-tests at CERN with a 120 GeV pion beam**

The mechanics

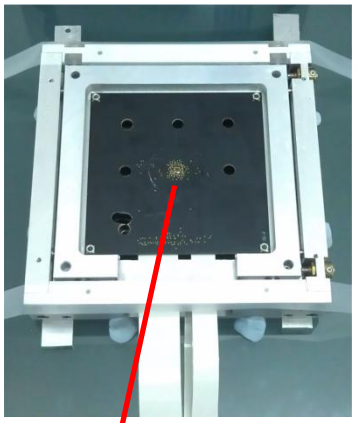

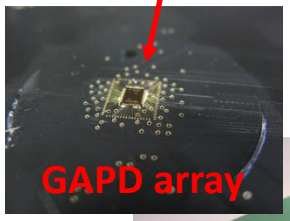

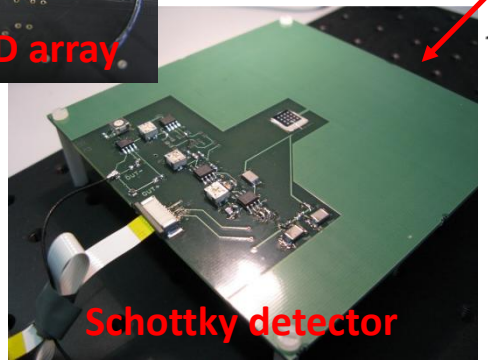

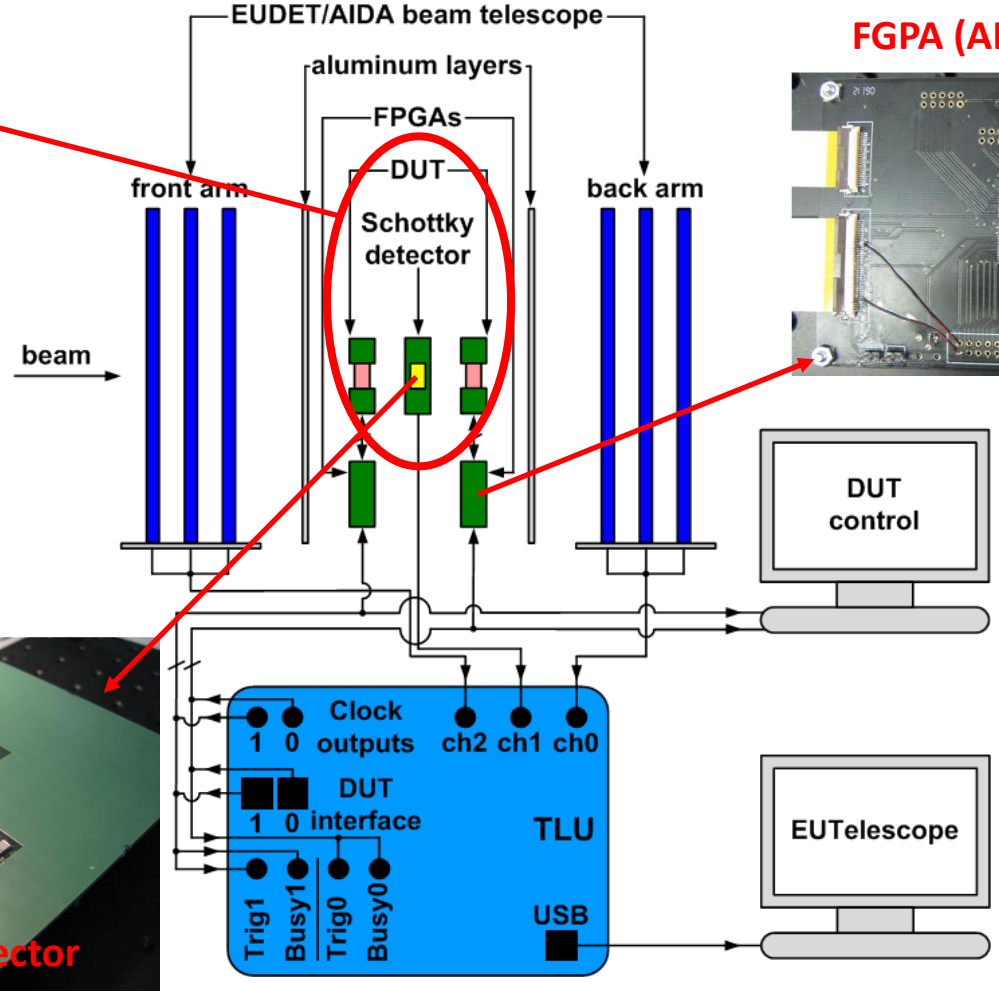

FGPA (ALTERA Cyclone IV)

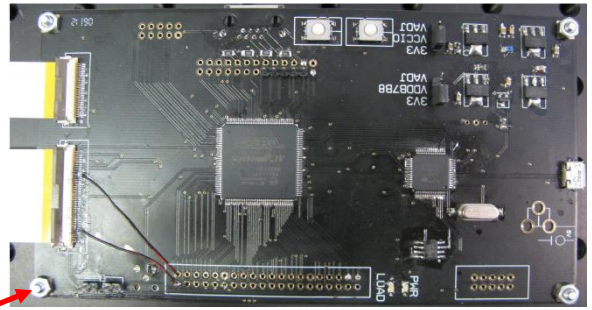

Special features to <u>avoid multiscattering</u>:

- Wafer of 250 µm
- No chip package
- PCB drilled under chip

E. Vilella et al., A test beam set-up for the characterization of the Geiger-mode avalanche photodiode technology for particle tracking , NIM A 694, 2012

High energy particle detection (2)

- **Set-up used at CERN**

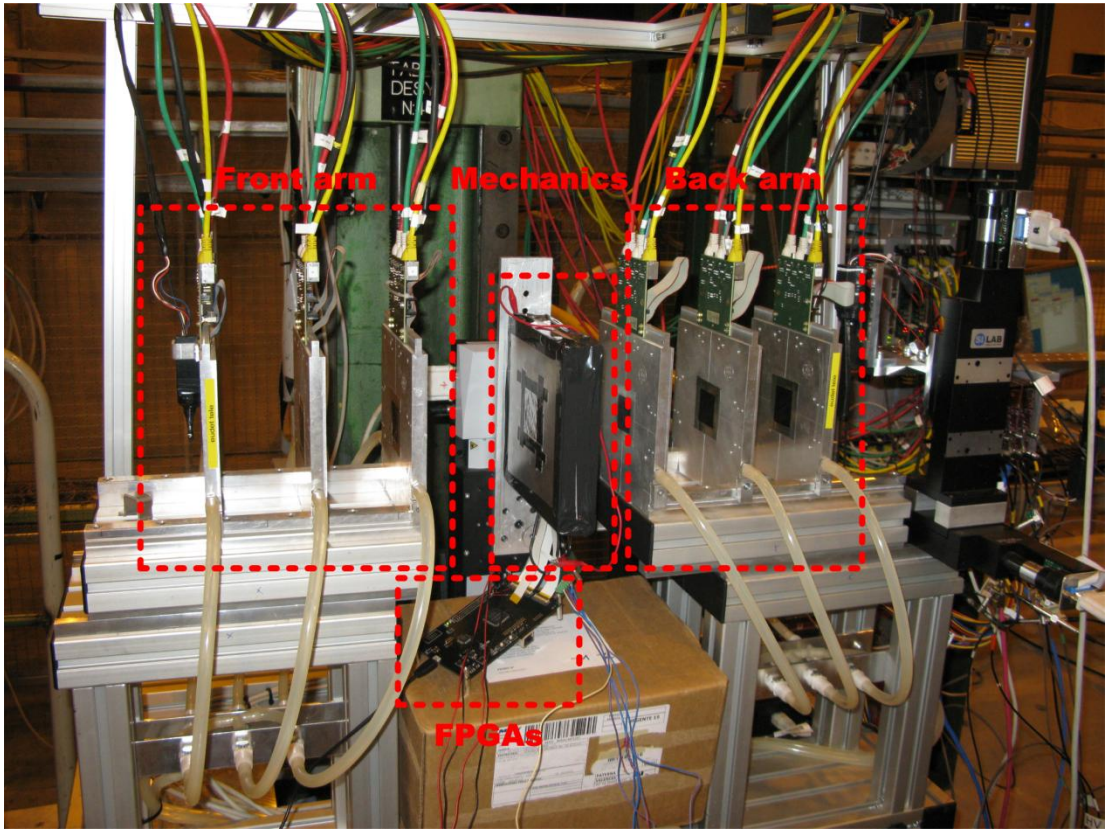

Correlation between the GAPD detector array and the EUDET/AIDA beam telescope (t_{on}=30 ns, V_{OV}=1.2 V)

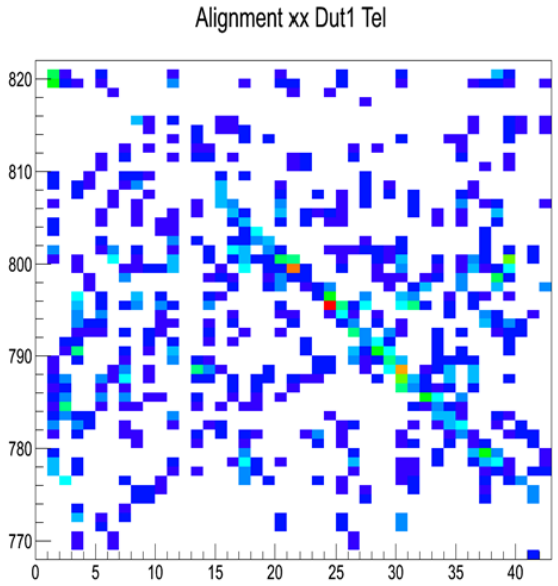

J. Trenado *et al.*, "Geiger-mode devices for charged particle tracking", presented at *IX Jornadas sobre la participación española en futuros aceleradores lineales*, Valencia, Spain, 2012.

Noise, Advantages of time-gated operation (1)

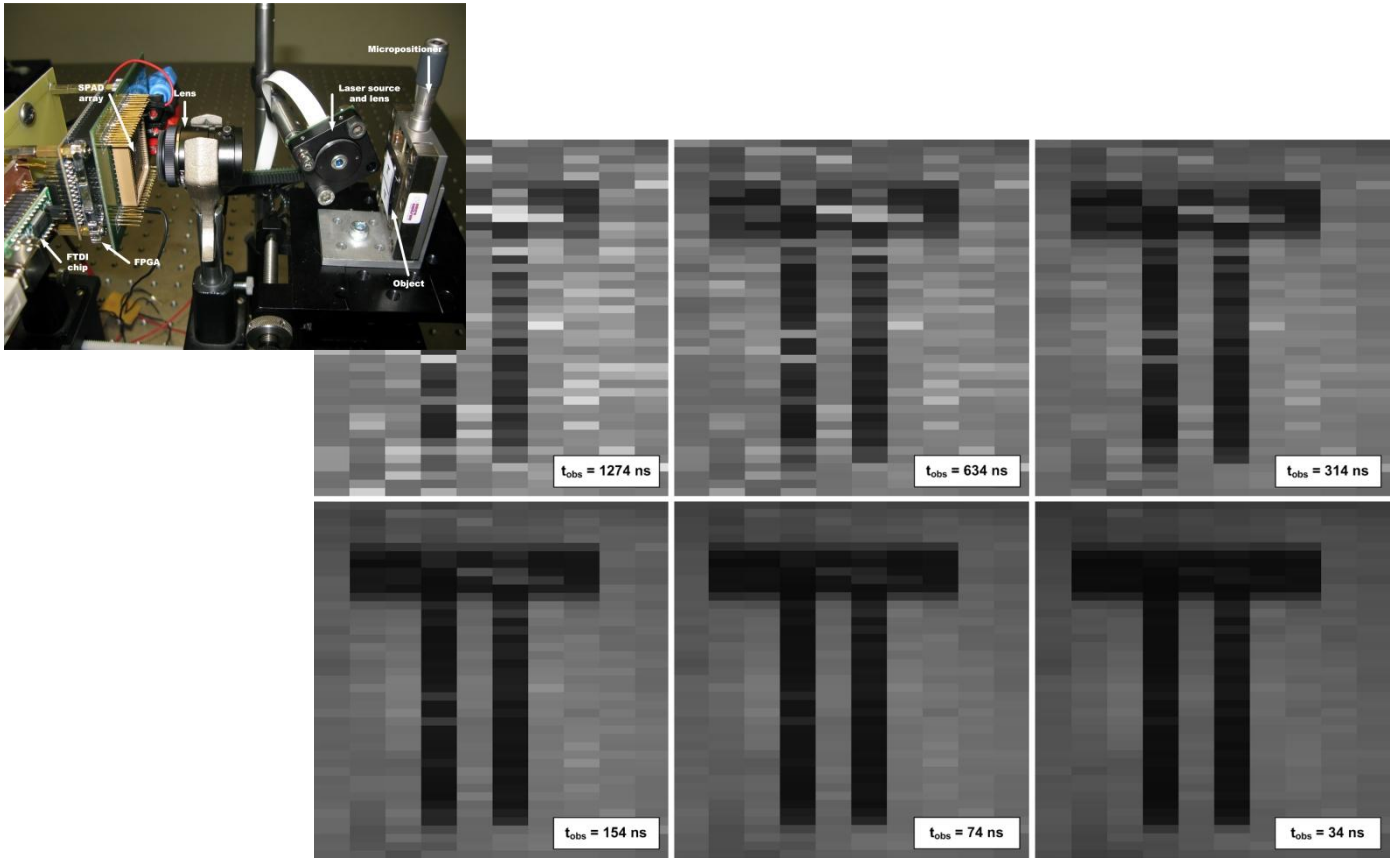

E. Vilella et al., A low-noise time-gated single-photon detector in a HV-CMOS technology for triggered imaging , Sensors &Actuators A 201, 2013.

- **From our experience with time-gated pixels (HV-AMS 0.35µm)**
  - elimination of afterpulses with periods (t_{OFF}) around

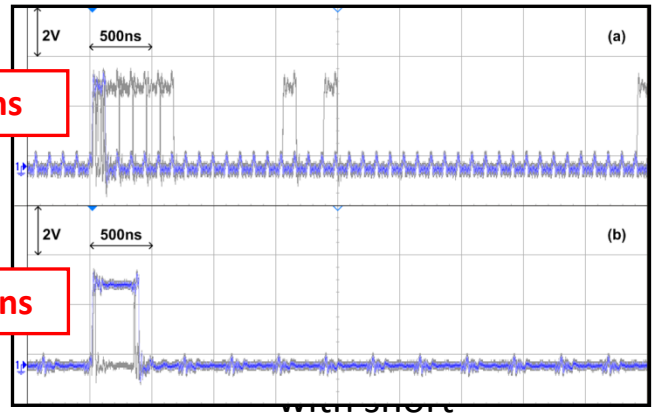

t_{OFF} = 80ns

t_{OFF} = 300ns

  - reduction of the detected dark counts active periods (t_{ON})

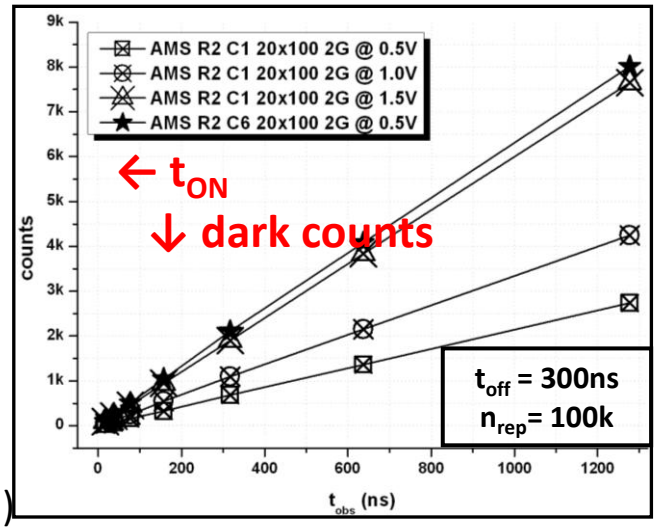

noise rate (in Hz) = (noise counts) / (t_{ON} x repetitions)

  - elimination of crosstalks with short active periods (t_{ON})

E. Vilella et al., DTIP 2013

Noise, Advantages of time-gated operation, T effects (3)

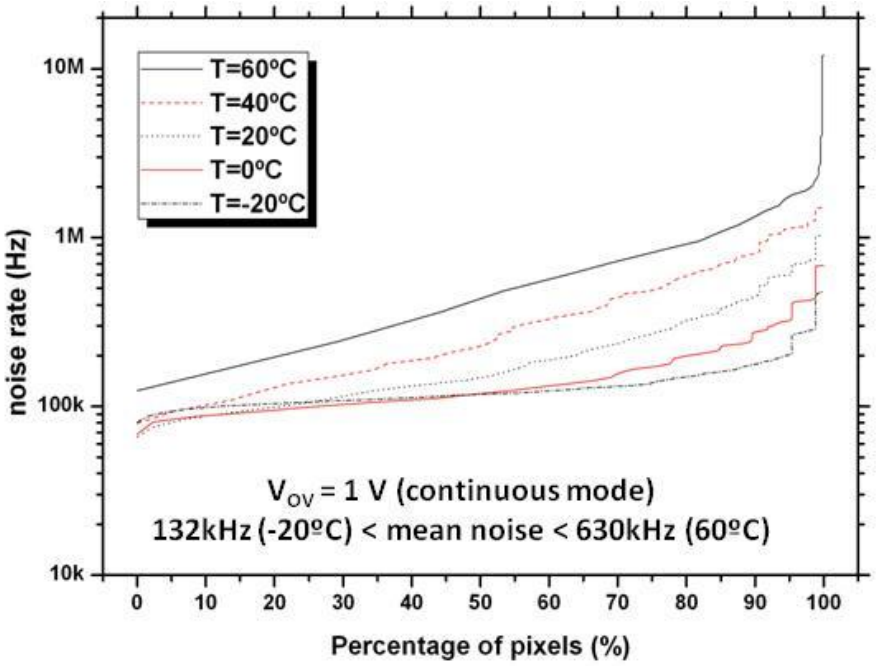

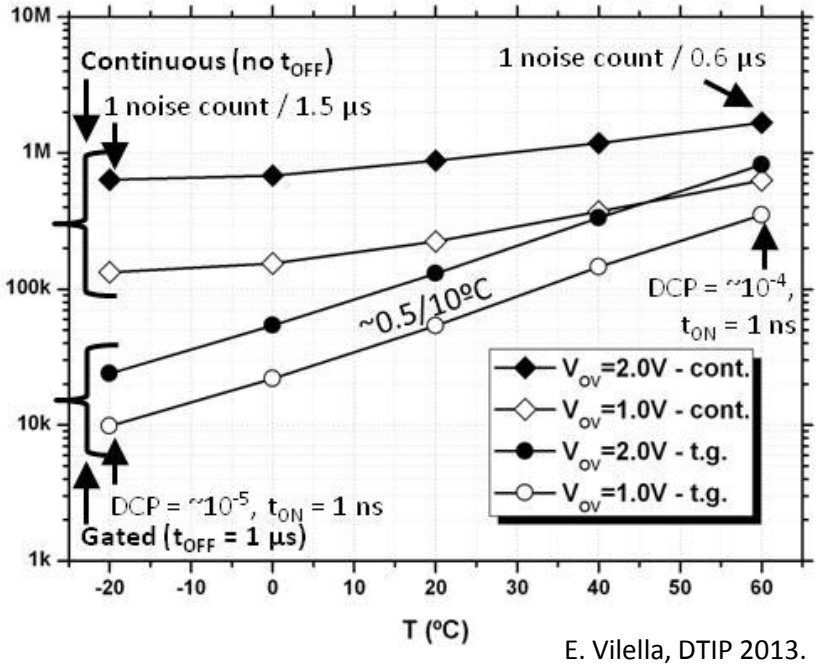

E. Vilella, DTIP 2013.

Better conditions for low noise:

- a nanosecond scale time-gated operation
- low working temperature

DCP (Dark Count Probability) = probability to detect 1 dark count in a given frame

DCP = noise rate x t_{ON}

T (ºC)	NCR/DCR (kHz)	Expected noise counts	
		ILC (2820BX, 337 ns)	CLIC (312 BX, 0.5 ns)
60	630 (NCR)	598 n.c./GAPD/train	0.1 n.c./GAPD/train
	350 (DCR)	$3 \cdot 10^{-3}$ n.c./GAPD/BX (t_{obs}=10 ns) $3 \cdot 10^{-4}$ n.c./GAPD/BX (t_{obs}=1 ns)	– –
-20	132 (NCR)	125 n.c./GAPD/train	0.02 n.c./GAPD/train
	9.8 (DCR)	10^{-4} n.c./GAPD/BX (t_{obs}=10 ns) 10^{-5} n.c./GAPD/BX (t_{obs}=1 ns)	– –

Table 4.1 Expected noise counts at ILC and CLIC as a function of the temperature at 1 V of V_{OV}.

E. Vilella, PhD 2013.

Noise, effects of radiation (4)

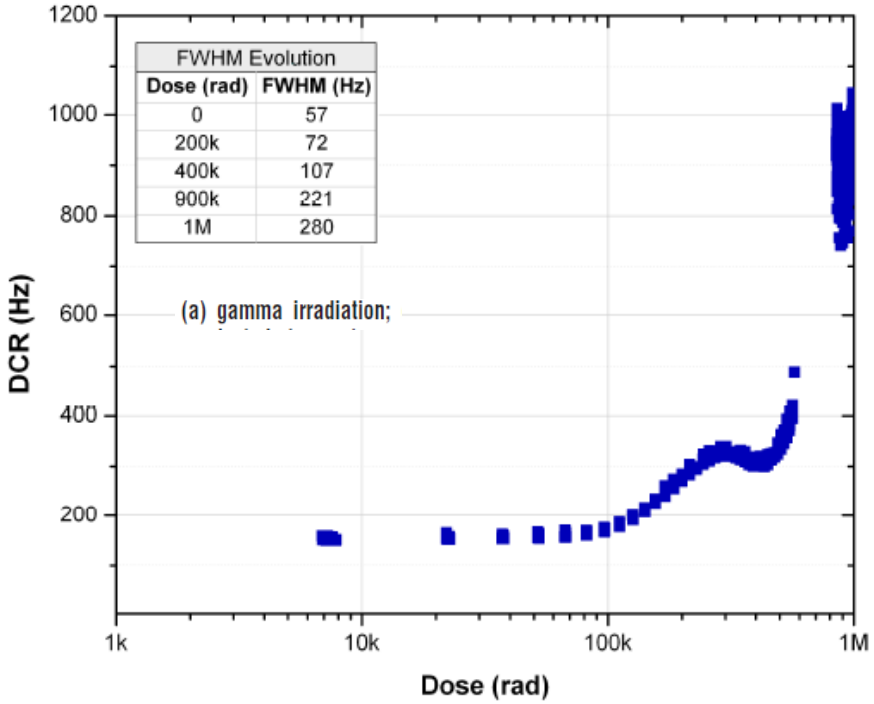

L. Carrara et al., "A gamma, X-ray, and high energy proton radiation-tolerant CIs for space applications", *IEEE Intl. Solid-State Circuits Conference*, pp. 40-42, 2009.

Irradiation type	Source	Fluence/ Flux	Dose (Si)	Initial DCR	Final DCR	DCR after Annealing (anneal time)
Gamma	Co60	10.46rad/min	1.0Mrad	153	1020	276 (172h)
X	Comet-Yxlon TU320-D03	4.3AsV²	0.25mGy	540	545	540 (1min)
		324AsV²	0.25mGy	540	640	540 (1min)
		900AsV²	0.5mGy	540	701	540 (1min)
Proton	Accelerator	1.8x10⁷p/cm²/s (11MeV)	40.0krad	140	6298	3884 (10d)
		8.3x10⁷p/cm²/s (60MeV)	40.0krad	142	6290	1299 (21d)

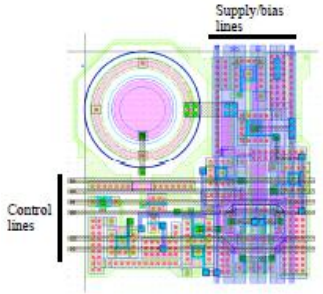

Pixel of C. Niclass et al., "A Single-photon Avalanche Diode Array Fabricated in 0.35µm CMOS and Based on an Event-Driven Readout for TCSPC Experiments", Proc. SPIE, vol. 6372, Oct. 2006.

Fill factor (1)

- Fill-factor > 90% required
- In our 0.35µm HV-AMS standard CMOS process
  - p-n junctions (20µm×100µm)
  - Very simple readout
  - In the same n well to improve the fill factor (67%)

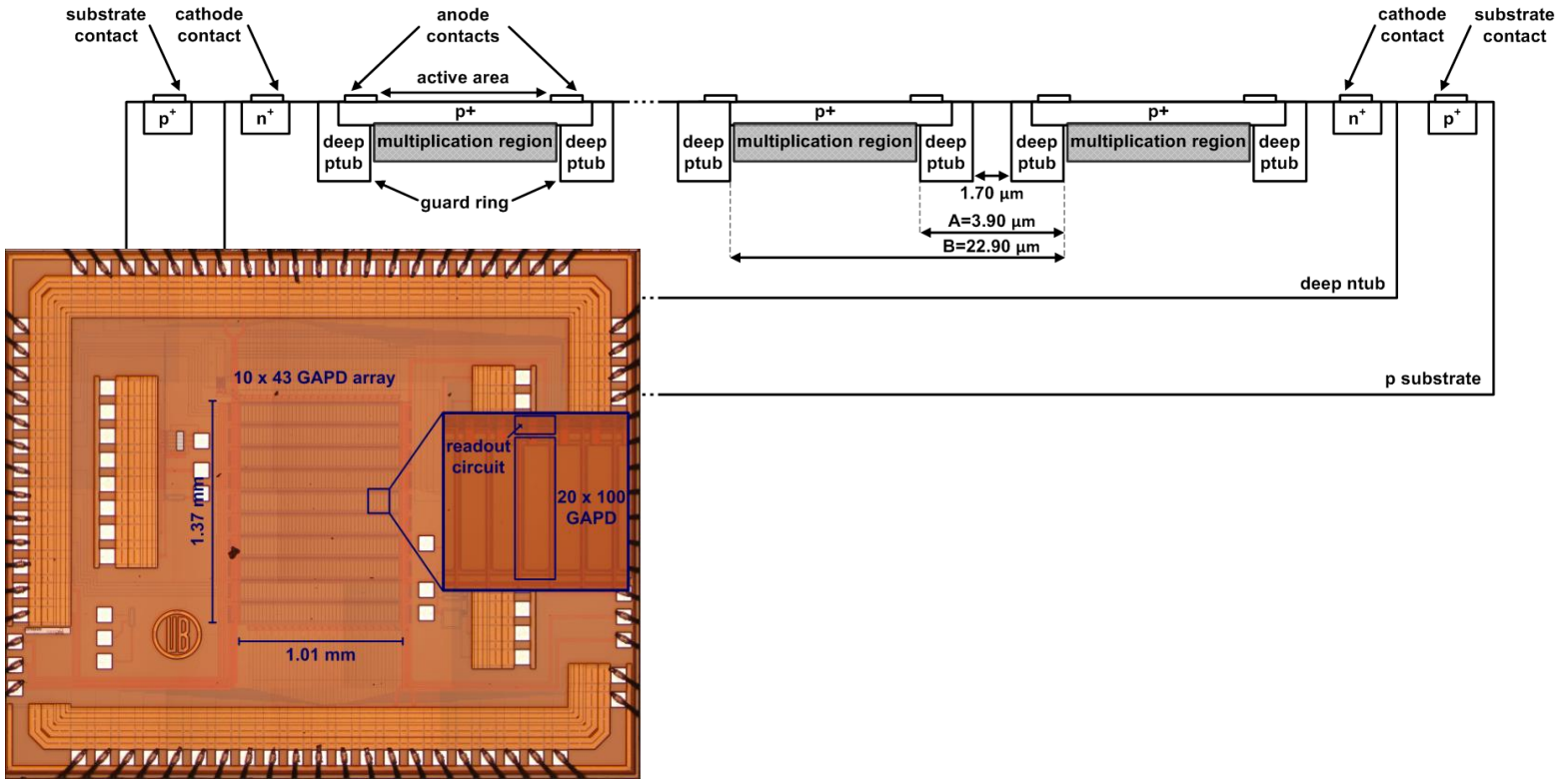

Fill factor (2)

- 3D-IC technologies as a solution to increase the fill-factor in GAPD arrays
  - Process → Chartered 130nm/Tezzaron 3D
  - 2-layer stack with TSVs (Through Silicon Vias) in a via first process
  - TSVs → SuperContacts with a recommended spacing of 100µm (dummy TSVs)
  - The 2 dies are connected face-to-face
  - I/O pads on the back of WTOP
- Our design

  T1 → sensors; T2 → sensors & electronics (the dead areas of one tier are overlapped by the active areas of the other tier)
  - Sensor size → 18µm x 18µm, 30µm x 30µm
  - Time-gated operation
  - Passive quenching, active recharge/inhibit

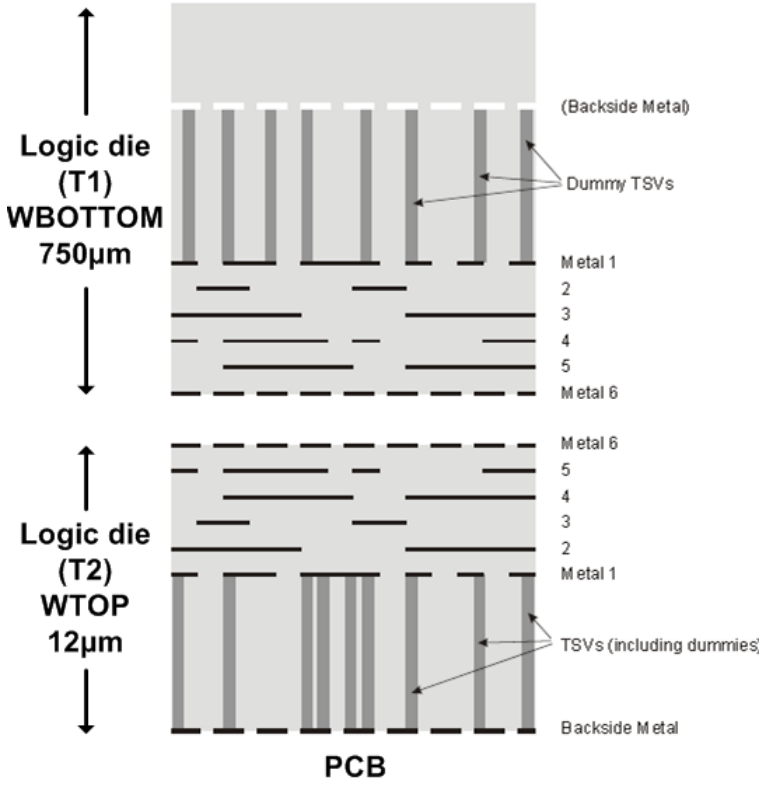

Fill factor (3)

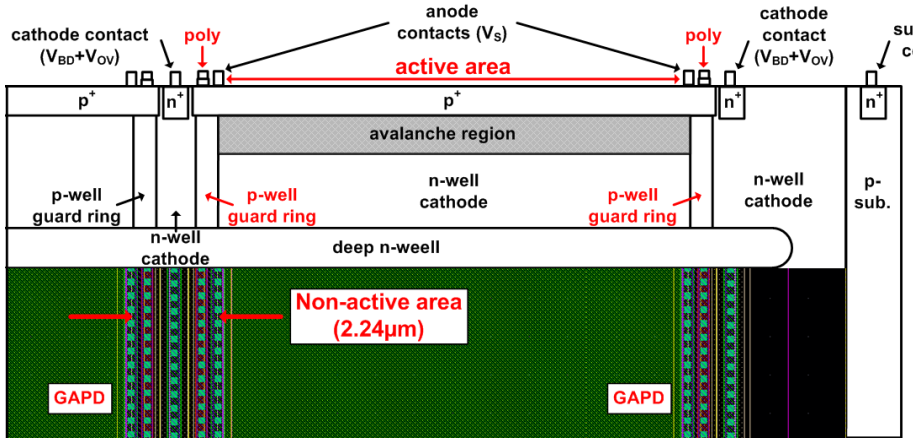

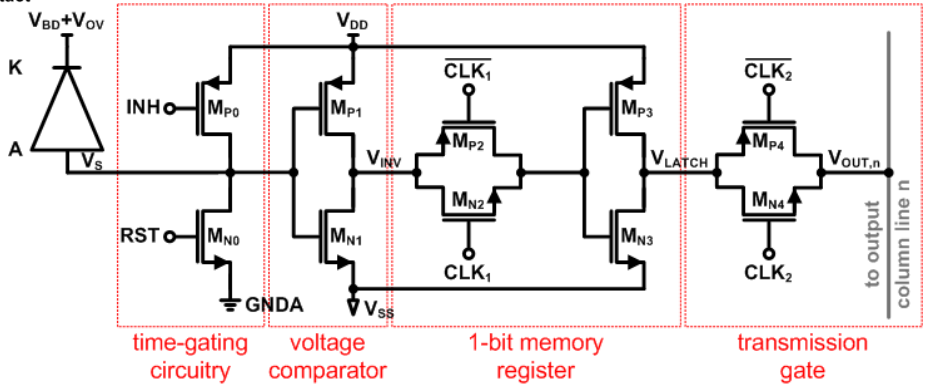

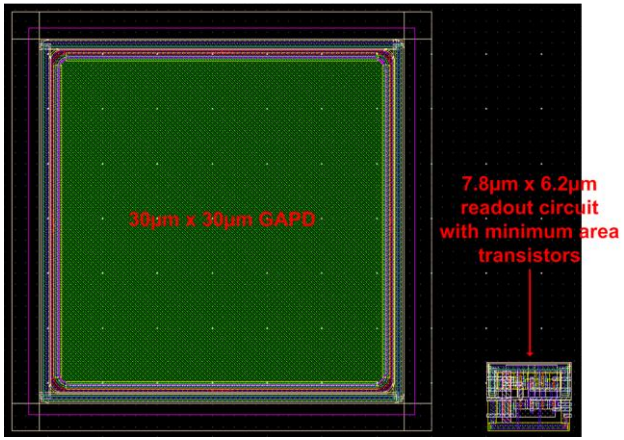

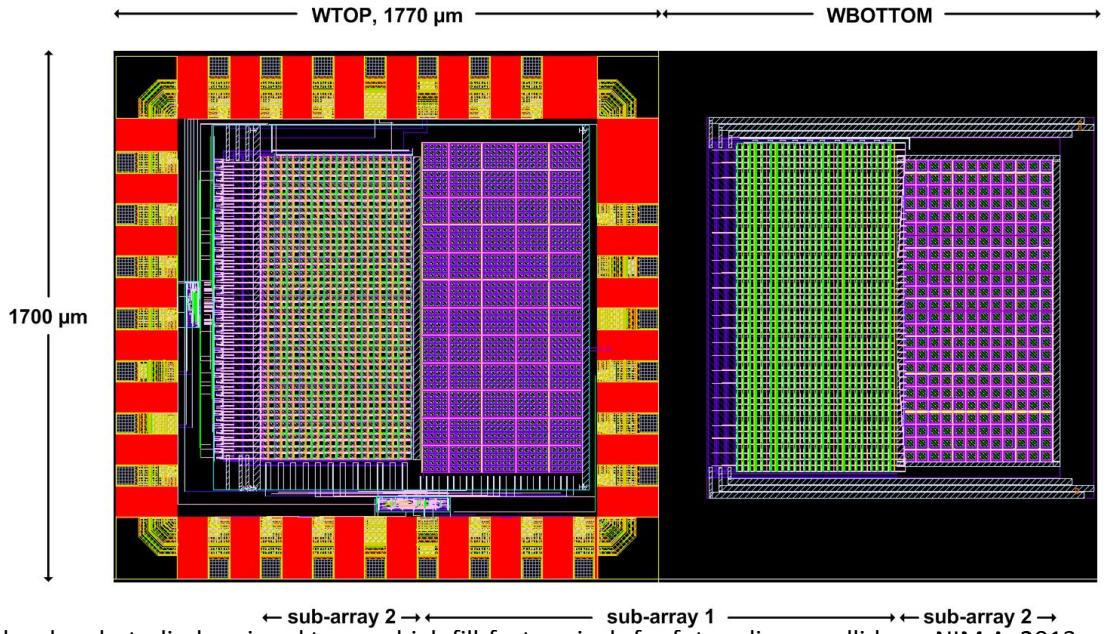

E. Vilella et al., 3D integration of Geiger-mode avalanche photodiodes aimed to very high fill-factor pixels for future linear colliders , NIM A, 2013

Fill factor (4)

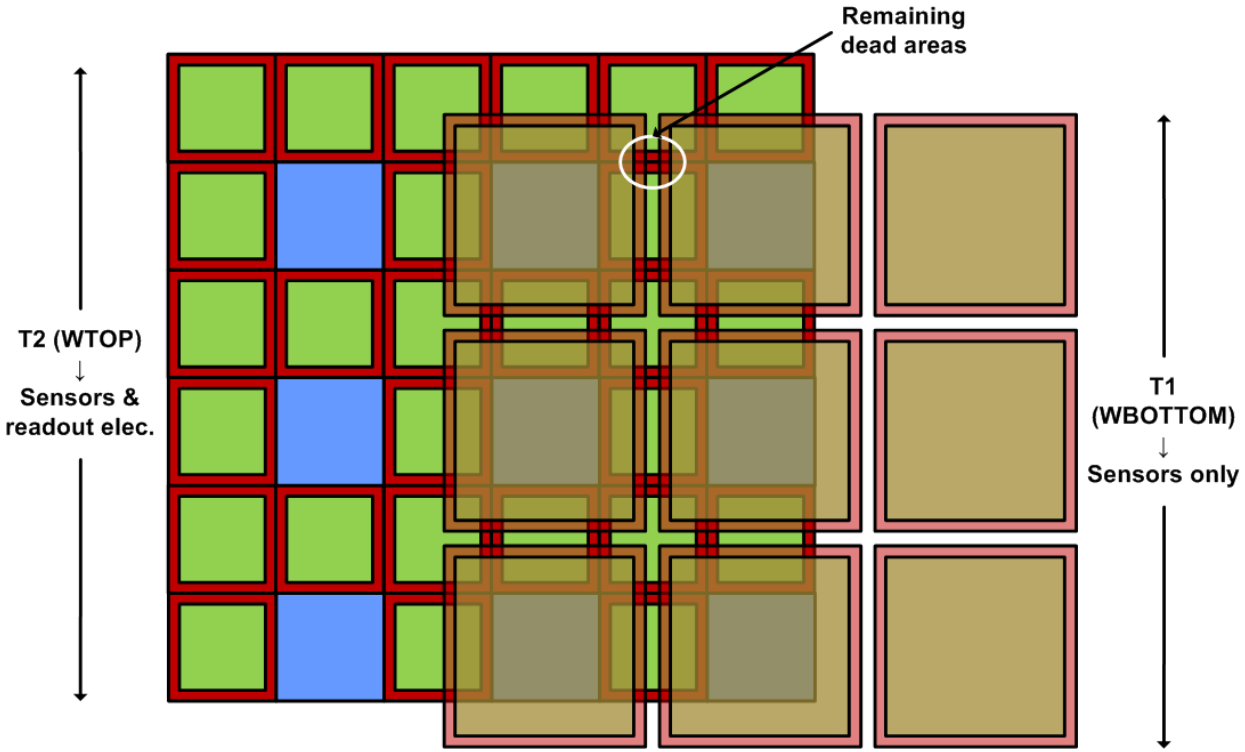

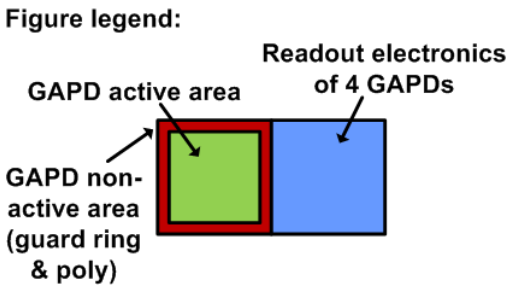

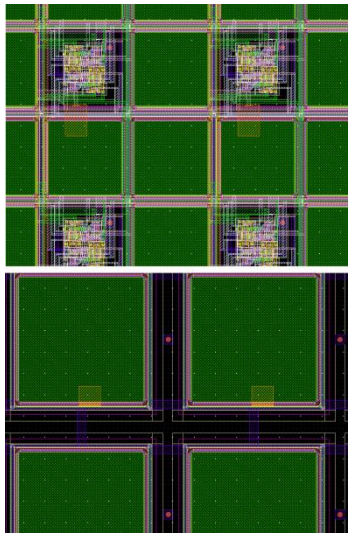

- T1 → sensors; T2 → sensors & electronics
- Array size → 48 rows x 24 columns
- Sensor size → 18μm x 18μm (T1), 30μm x 30μm (T2)
- Interconnection between tiers → 30μm x 30μm GAPD to its readout circuit
- Fill-factor → **92%**

CONCLUSIONS

All the elements to achieve the ideal tracker (always fires when particle arrives AND never fires when no particle arrives) seem to be there.

(1) integration -> CMOS,

(2) low noise for some processes and structures, gating, cooling,

(3) fill factor with 3D/bonding hybrids.

However, it is still needed a lot of effort focused to a particular detector to combine all.

At this moment seems a promising technology, also for HEP

…considering a GAPD pixel with a sensitive area of 20m x 100µm,
Background VX ILC (L1) ~10^{-4} hits/GAPD/BX, FTD ILC (L4) ~10^{-7} hits/GAPD/BX.
Noise sensor ~10^{-5} noise counts/GAPD/BX, V_{OV}=1V, ton/off=1ns/300 ns, -20ºC. FF 67%.
Area (÷5), Better CMOS structure 1Hz/µm^2 (÷30), 3D (FF > 90%), ANDing (÷ 10^{-5}).

backup

$V_{BD}(T)$

- The SPAD is biased at a positive $V_{HV} = V_{BD} + V_{OV}$ (cathode)
- The pulses are sensed at the sensor anode
- V_{BD} falls with the temperature (thermal dependence of the ionization coefficients)
- To measure the sensor noise at a fixed V_{OV}, it is necessary to know $V_{BD}(T)$
- Data obtained with an SPAD accessible to the sensing node + a 4-wire method:

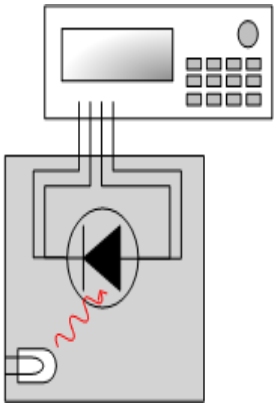

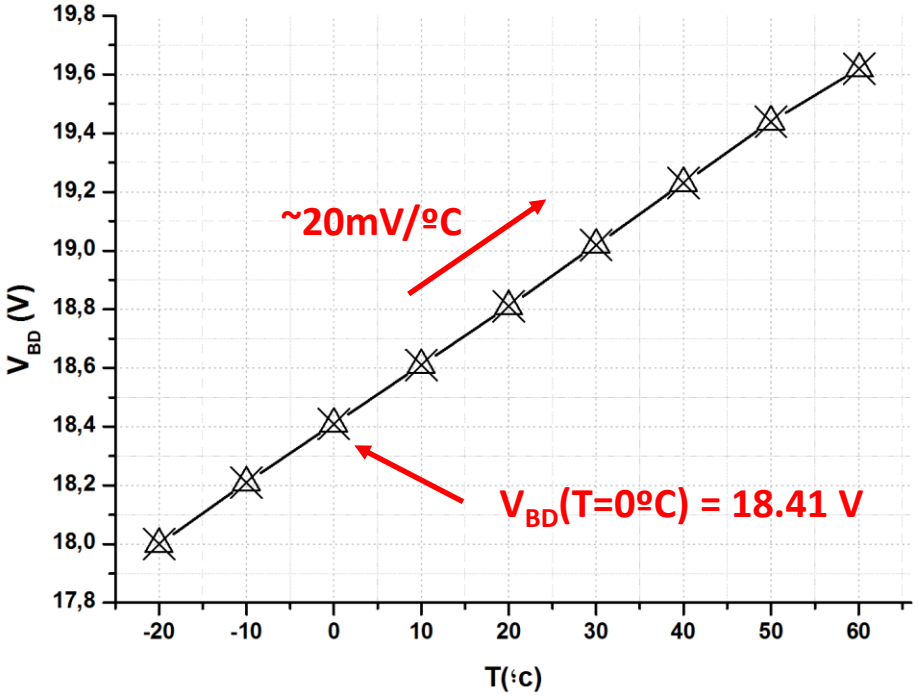

Table III-5.4. Pair induced backgrounds in the subdetectors for nominal 500 GeV and 1 TeV collision parameters [380]. The numbers for the ECAL and the HCAL are summed over barrel and endcaps. F detecor, the double-layer option has been chosen for this simulation. The TPC hits are the digitised h be written to the data acquisition system. The errors represent the RMS of the hit number fluctuatio bunch crossing (BX) simulations.

Sub-detector	Units	Layer	500 GeV	1000 GeV
VTX-DL	hits/cm^2/BX	1	6.320 ± 1.763	11.774 ± 0.992
		2	4.009 ± 1.176	7.479 ± 0.747
		3	0.250 ± 0.109	0.431 ± 0.128
		4	0.212 ± 0.094	0.360 ± 0.108
		5	0.048 ± 0.031	0.091 ± 0.044
		6	0.041 ± 0.026	0.082 ± 0.042
SIT	hits/cm^2/BX	1	0.0009 ± 0.0013	0.0016 ± 0.0016
		2	0.0002 ± 0.0003	0.0004 ± 0.0005
FTD	hits/cm^2/BX	1	0.072 ± 0.024	0.145 ± 0.024
		2	0.046 ± 0.017	0.102 ± 0.016
		3	0.025 ± 0.009	0.070 ± 0.009
		4	0.016 ± 0.005	0.046 ± 0.007
		5	0.011 ± 0.004	0.034 ± 0.005
		6	0.007 ± 0.004	0.024 ± 0.006
		7	0.006 ± 0.003	0.022 ± 0.006
SET	hits/BX	1	0.196 ± 0.924	0.588 ± 2.406
		2	0.239 ± 1.036	0.670 ± 2.616
TPC	hits/BX	-	216 ± 302	465 ± 356
ECAL	hits/BX	-	444 ± 118	1487 ± 166
HCAL	hits/BX	-	18049 ± 729	54507 ± 923

http://www.linearcollider.org/ILC/Publications/Technical-Design-Report, pag 282

Noise, deep-well structures are very low noise (~Hz/µm²)

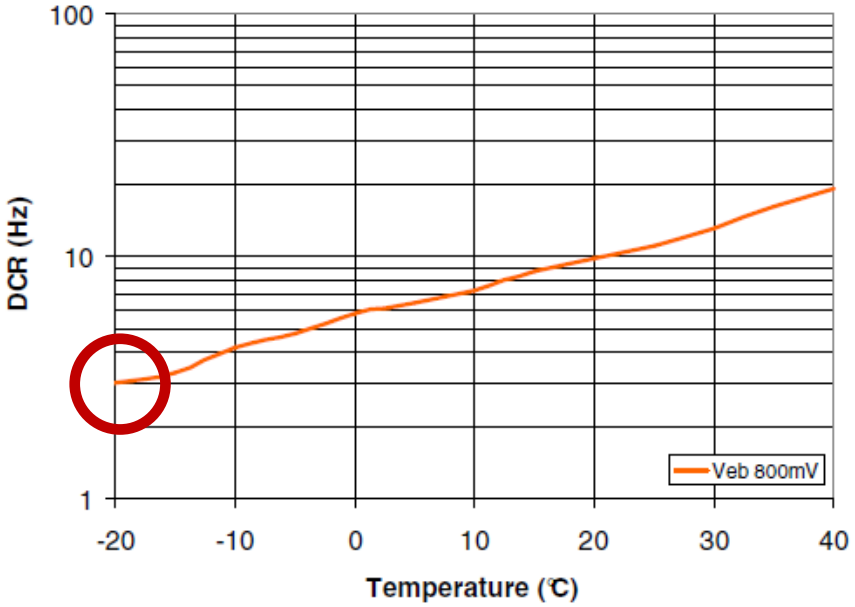

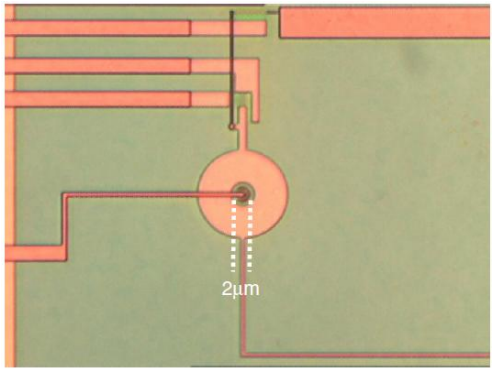

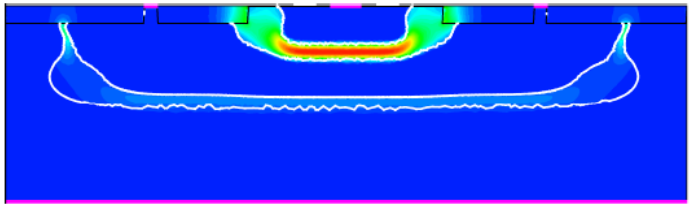

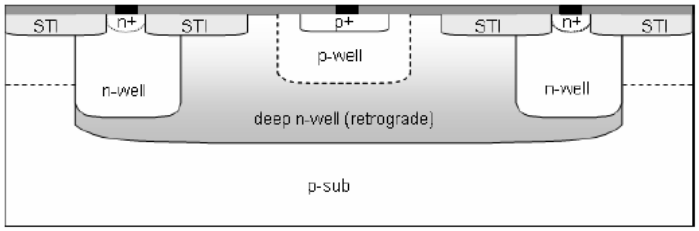

J. Richardson, L. A. Grant, and R. K. Henderson, "Low dark count single-photon avalanche diode structure compatible with standard nanometer scale CMOS technology," *IEEE Photon. Technol. Lett., vol. 21, no. 14,* pp. 1020–1022, Jul. 2009.

Noise, Advantages of 3D integration, layer ANDing

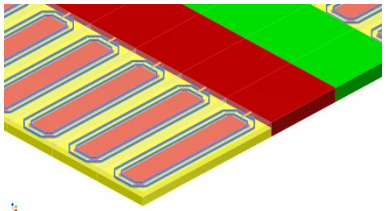

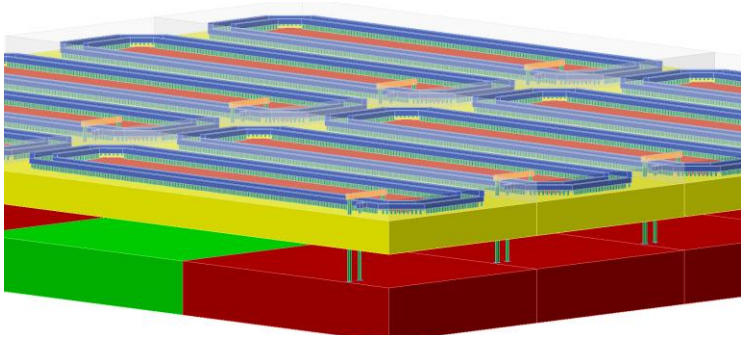

- The simplest idea…

  …gives the better interconnect performances

  …allows more complex pixel and inter-pixel processing and storage

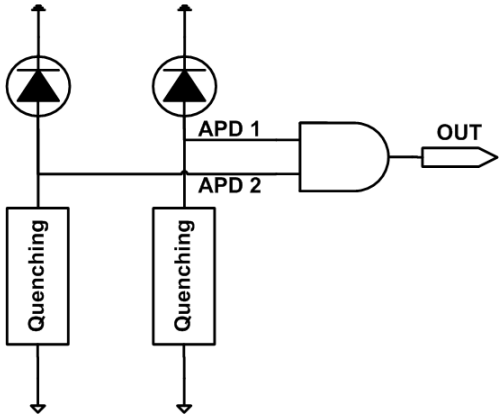

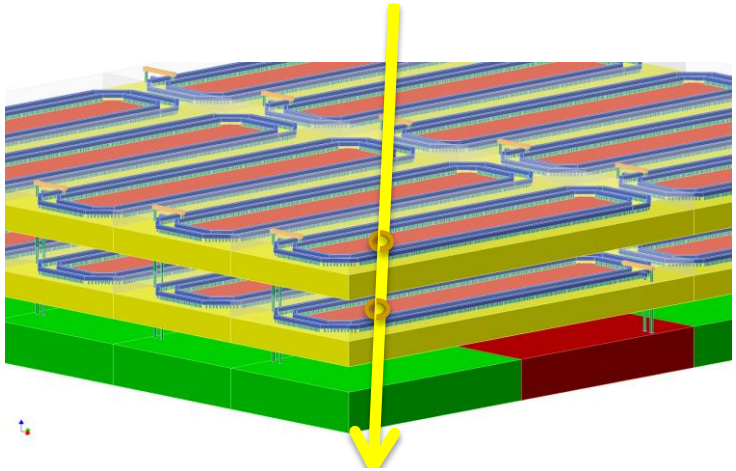

- Dark Count hits can be dramatically decreased with 3D technologies.

Fill Factor Issue with SPAD Sensors

Ref.	Array size	Technology	Pixel pitch	Fill Factor	In-pixel circuit
[1]	128x128	0.35um HV	25um	6%	Inverter + active quenching transistors (TDC at column level)
[2]	60x48	0.35um HV	85um	0.5%	2 gated counters
[3]	128x96	130nm CIS	44.6um	3.2%	Time-Of Flight extraction circuit
[4]	160x128	130nm CIS	50um	1%	Time-to-Digital Converter
[5]	3x3	90nm CIS	5um	12.5%	Inverter + passive quenching (3T)

[1] C. Niclass et al., ISSCC 2008
[2] C. Niclass et al., ESSCIRC 2008
[3] R. Walker et al., ISSCC 2011
[4] C. Veerappan et al., ISSCC 2011
[5] R.K. Henderson et al., IEDM 2010

Fill-factor, hybrid (custom APDs, bump bonded ASICs)

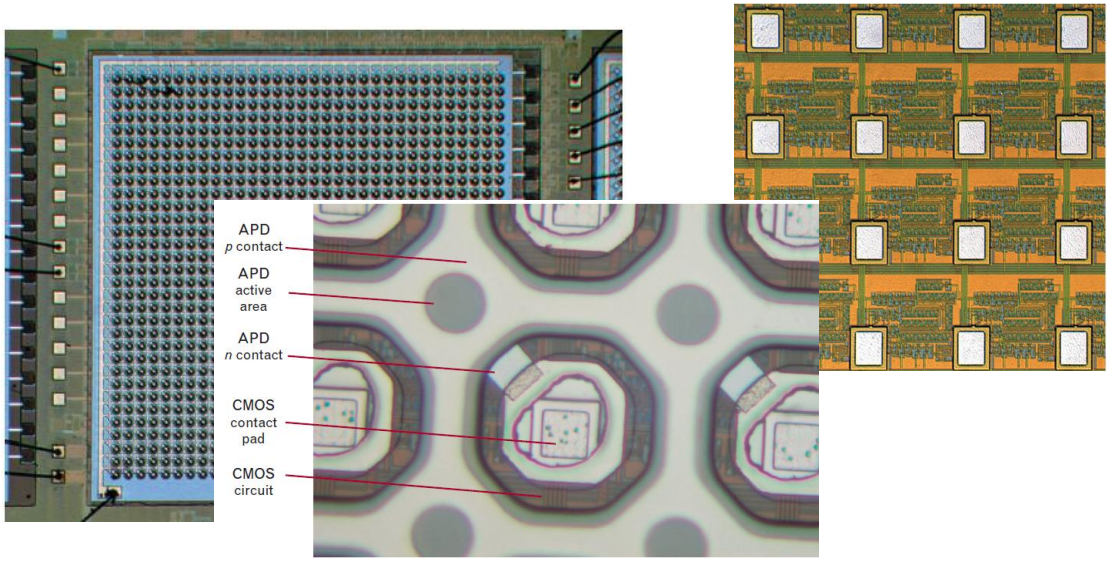

Brian F. Aull et al. , "Geiger-Mode Avalanche Photodiodes for Three-Dimensional Imaging" Proceedings of the SPIE, Volume 5353, pp. 105-116 (2004).

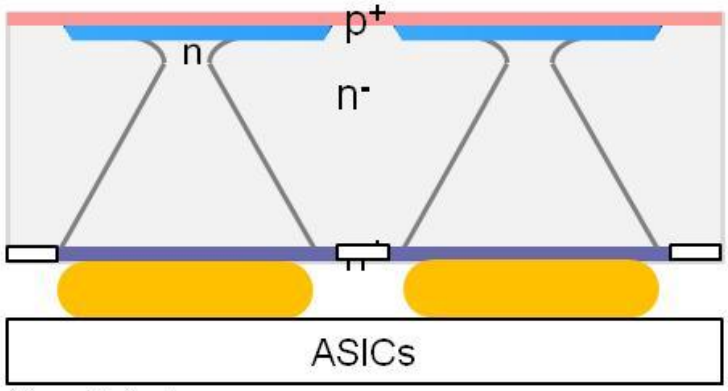

Jelena Ninkovic

Alternative solutions (HV-AMS)

- **Standard technology HV-AMS 0.35µm**

In this particular technology, and with our structure, the guard ring is sensitive → ≈ 100% fill-factor seems feasible (2)

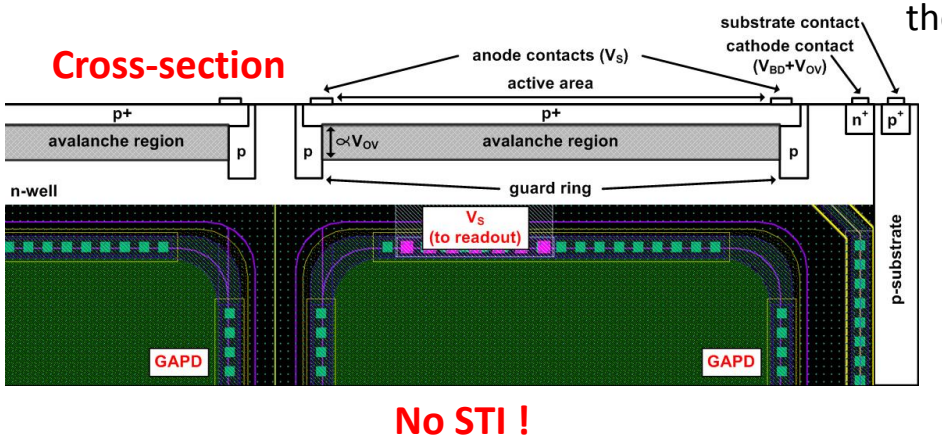

No STI !

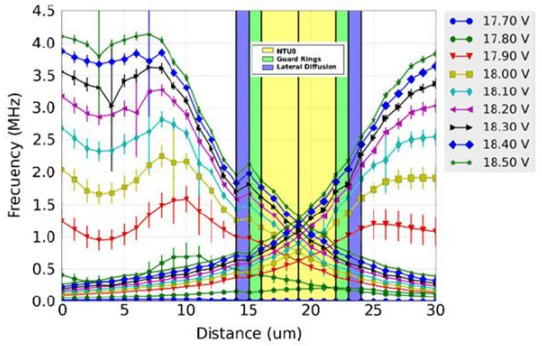

Fig. 16. Detection frequencies measured by scanning a 30 keV electron beam onto two neighbouring pixels in the array.

- **2-layer stack → Possible structures**

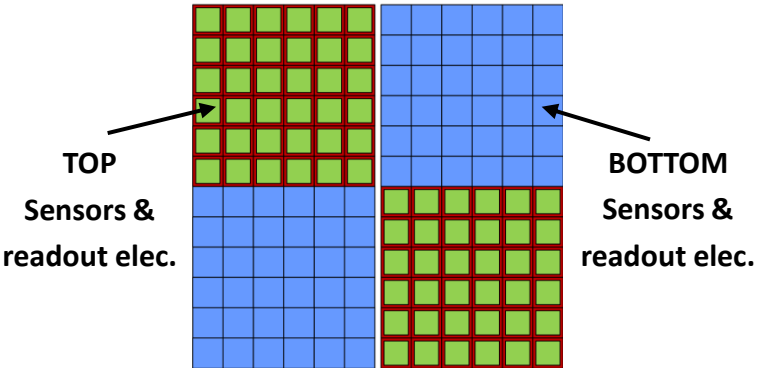

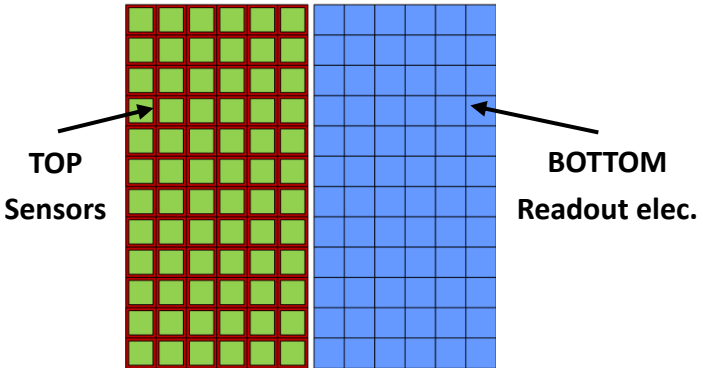

(2) A. Vilà, Characterization and simulation of avalanche photodiodes for next-generation colliders, Sens. Actuators A (2011).